

Identification of Palmitoyl Protein Thioesterase 1 in Human THP1 Monocytes and Macrophages and Characterization of Unique Biochemical Activities for This Enzyme

Ran Wang,^{†,‡} Abdolsamad Borazjani,[†] Anberitha T. Matthews,[†] Lee C. Mangum,[†] Mariola J. Edelmann,[§] and Matthew K. Ross^{*,†}

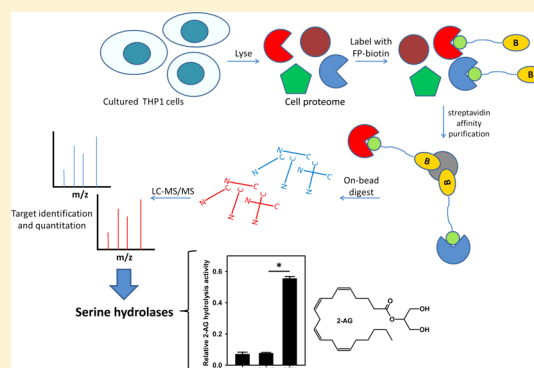
[†]Center for Environmental Health Sciences, Department of Basic Sciences, College of Veterinary Medicine, Mississippi State University, University, Mississippi 39762, United States

[‡]Institute of Food Safety, Jiangsu Academy of Agricultural Sciences, Nanjing 210014, China

[§]Institute for Genomics, Biotechnology, and Bioinformatics, Mississippi State University, University, Mississippi 39762, United States

S Supporting Information

ABSTRACT: The profiles of serine hydrolases in human and mouse macrophages are similar yet different. For instance, human macrophages express high levels of carboxylesterase 1 (CES1), whereas mouse macrophages have minimal amounts of the orthologous murine CES1. On the other hand, macrophages from both species exhibit limited expression of the canonical 2-arachidonoylglycerol (2-AG) hydrolytic enzyme, MAGL. Our previous study showed CES1 was partly responsible for the hydrolysis of 2-AG (50%) and prostaglandin glyceryl esters (PG-Gs) (80–95%) in human THP1 monocytes and macrophages. However, MAGL and other endocannabinoid hydrolases, FAAH, ABHD6, and ABHD12, did not have a role because of limited expression or no expression. Thus, another enzyme was hypothesized to be responsible for the remaining 2-AG hydrolysis activity following chemical inhibition and immunodepletion of CES1 (previous study) or CES1 gene knockdown (this study). Here we identified two candidate serine hydrolases in THP1 cell lysates by activity-based protein profiling (ABPP)—MUDPIT and Western blotting: cathepsin G and palmitoyl protein thioesterase 1 (PPT1). Both proteins exhibited electrophoretic properties similar to those of a serine hydrolase in THP1 cells detected by gel-based ABPP at 31–32 kDa; however, only PPT1 exhibited lipolytic activity and hydrolyzed 2-AG *in vitro*. Interestingly, PPT1 was strongly expressed in THP1 cells but was significantly less reactive than cathepsin G toward the activity-based probe, fluorophosphonate-biotin. KIAA1363, another serine hydrolase, was also identified in THP1 cells but did not have significant lipolytic activity. On the basis of chemoproteomic profiling, immunodepletion studies, and chemical inhibitor profiles, we estimated that PPT1 contributed 32–40% of 2-AG hydrolysis activity in the THP1 cell line. In addition, pure recombinant PPT1 catalyzed the hydrolysis of 2-AG, PGE₂-G, and PGF_{2α}-G, although the catalytic efficiency of hydrolysis of 2-AG by PPT1 was ~10-fold lower than that of CES1. PPT1 was also insensitive to several chemical inhibitors that potently inhibit CES1, such as organophosphate poisons and JZL184. This is the first report to document the expression of PPT1 in a human monocyte and macrophage cell line and to show PPT1 can hydrolyze the natural substrates 2-AG and PG-Gs. These findings suggest that PPT1 may participate in endocannabinoid metabolism within specific cellular contexts and highlights the functional redundancy often exhibited by enzymes involved in lipid metabolism.



The endogenous cannabinoid system is comprised of several components, including two distinct G-protein-coupled receptors (CB1 and CB2), the endogenous arachidonoyl-containing ligands 2-arachidonoylglycerol (2-AG) and anandamide (AEA), and enzymes responsible for 2-AG and AEA biosynthesis and inactivation.¹ The CB1 receptor is expressed primarily in the central nervous system (CNS) and to a more limited extent in peripheral tissues and immune cells. On the other hand, CB2 is mainly expressed peripherally, particularly on immune cells such as macrophages, with smaller quantities found in the brain.^{2,3} Therefore, activation of CB1

and CB2 receptors by both endogenous and exogenous cannabinoids has several well-characterized central and peripheral effects.³ The two widely studied endocannabinoids, 2-AG and AEA, are produced on demand and act locally in a paracrine and autocrine manner, and their physiological actions are terminated by hydrolytic enzymes that reduce their local concentration. The balance between biosynthesis and degrada-

Received: August 19, 2013

Revised: September 30, 2013

Published: October 1, 2013



tion of endocannabinoids is often altered under pathological conditions, and an imbalance can modulate the actions of these bioactive lipids.^{1,4} Therefore, the local concentration of 2-AG in various niches may be an important determinant of disease development. For example, endocannabinoids released from endothelial cells, macrophages, and platelets play a critical role in atherogenesis and can partially contribute to its clinical manifestations.⁵

In cells, 2-AG is synthesized from arachidonoyl-containing membrane lipids by an *sn*-1-specific diacylglycerol lipase (DAGL α or β). Following production in the CNS, 2-AG is primarily degraded (~80%) by monoacylglycerol lipase (MAGL),¹ although α/β hydrolases ABHD6 and ABHD12 also make contributions.^{6–9} Though much is known about 2-AG-mediated retrograde neurotransmission and how 2-AG is metabolized in the brain, far less is known about the physiological actions of 2-AG in peripheral tissues, such as macrophages, and its catabolism. We previously showed that in certain cellular contexts 2-AG can be degraded by carboxylesterase 1 (CES1).¹⁰ CES1 is a well-known xenobiotic metabolizing enzyme expressed at high levels in human liver.¹¹ However, it is less well appreciated that CES1 is abundantly found in human macrophages^{12,13} but not in murine macrophages.¹³ In human macrophages, CES1 contributes to the liberation of free cholesterol from neutral lipid droplets, thus initiating the mobilization of cholesterol from macrophage foam cells for reverse cholesterol transport.^{12,14} In addition to 2-AG, CES1 can also hydrolyze prostaglandin glyceryl esters (PG-Gs),¹⁰ which are cyclooxygenase-derived oxygenated products of 2-AG.^{15,16} CES1 accounted for 40–50 and 80–95% of the 2-AG and PG-G hydrolysis activity, respectively, in the THP1 macrophage cell line. Furthermore, the catalytic efficiency of hydrolysis of 2-AG by CES1 was similar to that of MAGL. However, on the basis of Western blotting, MAGL was expressed in very small amounts in the THP1 cell line¹⁰ and could not be detected by activity-based protein profiling (ABPP)–MUDPIT (*vide infra*). It is noteworthy that *bona fide* 2-AG hydrolysis enzymes FAAH, ABHD6, and ABHD12 also could not be detected in THP1 cells by either Western blotting or a gel-based ABPP assay.¹⁰ Furthermore, the selective ABHD6 inhibitor WWL70¹⁷ did not block the 2-AG hydrolysis activity of THP1 cell lysates.¹⁰ These findings suggested that the remaining 2-AG hydrolysis activity in the cell line was not due to MAGL, FAAH, ABHD6, or ABHD12, which led us to examine other candidates.

When serine hydrolases in THP1 cells were labeled by the chemoproteomic probe fluorophosphonate-biotin (FP-biotin)¹⁸ and separated by sodium dodecyl sulfate–polyacrylamide gel electrophoresis (SDS–PAGE), it was found that CES1 and an uncharacterized protein (doublet at $M_r \sim 31$ –32 kDa) were the major hydrolases detected by avidin–horseradish peroxidase blotting.^{10,19} We initially considered the possibility that the uncharacterized enzyme was MAGL; however, two lines of evidence argued against this.¹⁰ (i) The protein was not immunoreactive toward a human MAGL antibody. (ii) Its catalytic activity was not inhibited by the potent MAGL inhibitor, JZL184, as judged by competitive gel-based ABPP in which inhibitors are evaluated for their ability to impair probe labeling of target serine hydrolases,²⁰ nor was it inhibited by the potent serine hydrolase inhibitors paraoxon and chlorpyrifos oxon, which are organophosphate poisons. Thus, we sought to identify this uncharacterized serine hydrolase. In the study presented here, the identities of two unknown serine hydrolases

in the THP1 cell line are reported for the first time: a serine protease (cathepsin G) and serine lipase [palmitoyl protein thioesterase 1 (PPT1)]. Because of their similar molecular masses (~30–34 kDa), both likely contribute to the signals detected by gel-based ABPP.^{10,19} Furthermore, we have confirmed by gene knockdown methods that CES1 is involved in 2-AG catabolism in intact THP1 monocytes and macrophages. Importantly, we characterized some unique hydrolytic activities for PPT1 that suggest it contributes to 2-AG hydrolysis in THP1 cells. Although PPT1 is known to hydrolyze fatty acyl groups attached to cysteine residues in proteins,²¹ we determined that PPT1 can also catalyze the hydrolysis of 2-AG and PG-Gs and that PPT1 may collaborate with CES1 to degrade 2-AG in THP1 monocytes and macrophages.

EXPERIMENTAL PROCEDURES

Chemicals, Cells, and Reagents. Authentic standards of 2-AG, 2-AG- d_8 , arachidonic acid (AA), AA- d_8 , prostaglandin E₂ glyceryl ester (PGE₂-G), prostaglandin F_{2 α} glyceryl ester (PGF_{2 α} -G), PGE₂, PGF_{2 α} , and 8-iso-PGF_{2 α} - d_4 were from Cayman Chemicals (Ann Arbor, MI). *p*-Nitrophenyl valerate (pNPV), 4-methylumbelliferyl acetate (4-MUBA), and 4-methylumbelliferyl oleate (4-MUBO) were from Sigma (St. Louis, MO). Paraaxon (PO) was a kind gift from H. Chambers (Mississippi State University). Hexadecylsulfonyl fluoride (HDSF) was purchased from Calbiochem. Trypan blue, β -mercaptoethanol, phorbol 12-myristate 13-acetate (PMA), methyl arachidonylfluorophosphonate (MAFP), fatty acid-free bovine serum albumin (BSA), penicillin, streptomycin, puromycin, and all buffer components were purchased from Sigma. The activity-based serine hydrolase probe, fluorophosphonate-biotin (FP-biotin), was from Toronto Research Chemicals (North York, ON). Streptavidin–agarose beads and avidin–horseradish peroxidase were from Sigma. High-performance liquid chromatography (HPLC) grade solvents were from Thermo-Fisher.

Human THP1 monocytes, HepG2 cells, RPMI-1640 medium, Dulbecco's modified Eagle's medium (DMEM), a gentamicin sulfate solution (50 mg/mL), and Hank's balanced salt solution without calcium, magnesium, or phenol red were purchased from American Type Culture Collection (ATCC) (Manassas, VA). Fetal bovine serum (FBS) was purchased from Invitrogen (Carlsbad, CA). Primary mouse macrophages were obtained from lavage of the peritoneal cavity of adult female B6C3F1 mice using sterile PBS containing 3% (v/v) FBS. Washed cells (PBS) were plated overnight in DMEM supplemented with 10% (v/v) FBS and antibiotics (penicillin and streptomycin) and adherent cells harvested. Primary human monocytes were commercially obtained from Astarte Biologics (Redmond, WA).

CHO-hPPT1 cells were a kind gift from S. Hofmann (University of Texas Southwestern Medical Center, Dallas, TX). Nucleoside-deficient minimal essential medium (Gibco), dialyzed FBS (Gemini), F-12 medium (Invitrogen), and serum-free medium (Hyclone CD4CHO) were obtained for culturing CHO-hPPT1 cells. Lentiviruses containing scrambled shRNA (nonspecific) and CES1 shRNA were from Santa Cruz Biotechnology.

Recombinant human CES1 was expressed in baculovirus-infected *Spodoptera frugiperda* cells and purified as previously described.²² Recombinant KIAA1363 was overexpressed in COS7 cells transfected with an expression vector containing

KIA1363 cDNA (Origene). Anti-CES1, anti-PPT1 antibody (ab89022), and anti- β -actin antibodies were purchased from Abcam (Cambridge, MA).

Culture Conditions. THP1 monocytes were grown in suspension of RPMI-1640 medium supplemented with 10% FBS, 0.05 mM β -mercaptoethanol, and 50 μ g/mL gentamicin (complete growth medium) at 37 °C in an atmosphere of 95% air and 5% CO₂. The cells were grown at a density between 0.2 \times 10⁶ and 1 \times 10⁶ cells/mL, as recommended by ATCC. THP1 monocytes were differentiated into macrophages by the addition of PMA to the culture medium (final concentration of 100 nM) for 48–72 h. The culture medium was replaced every 2 days with fresh PMA and growth medium.

Preparation of Cell Lysates. THP1 monocytes were collected by centrifugation (500g for 10 min at 4 °C), washed with cold phosphate-buffered saline (PBS), resuspended in ice-cold 50 mM Tris-HCl (pH 7.4) buffer, and lysed by sonication (four 15 s bursts on ice at 30% maximum power). THP1 macrophage monolayers were washed with cold PBS and scraped into cold 50 mM Tris-HCl (pH 7.4) buffer and sonicated. Protein concentrations of cell lysates were determined using the BCA reagent according to the manufacturer's instructions (Thermo-Fisher).

Primary mouse macrophages were plated in DMEM containing antibiotics (penicillin and streptomycin) and nonadherent cells removed after 3–4 h. Fresh medium was added, and the cells were cultured overnight. Adherent cells were washed with PBS, and the cells were scraped into ice-cold 50 mM Tris-HCl (pH 7.4) buffer and sonicated as described above.

Protease inhibitors and detergents were typically avoided when the hydrolytic activity of cell lysates was determined. In some cases, the cells were lysed in cold RIPA buffer containing protease inhibitors (Promega, catalog no. G6521) for subsequent immunoblot analysis.

Identification of Serine Hydrolases: On-Bead Digestion of Serine Hydrolases (ABPP–MUDPIT). THP1 monocyte lysate [2 mg/mL protein in 50 mM Tris-HCl (pH 7.4)] was incubated with the activity-based probe FP-biotin (final concentration of 8 μ M) for 1 h at room temperature, followed by removal of excess FP-biotin as previously described.¹⁴ This is termed the native sample. To control for nonspecific and noncatalytic labeling of proteins by FP-biotin, a separate, equivalent amount of lysate protein was heated for 5 min (90 °C) to denature proteins prior to the addition of FP-biotin. This is termed the heated sample. After the removal of excess FP-biotin, biotinylated proteins were captured by addition of washed streptavidin beads (150 μ L), followed by incubation on a rotator (room temperature for 3 h). The beads were subsequently washed with 5 mL of 0.2% (w/v) SDS in PBS once, 5 mL of PBS three times, and 5 mL of distilled water three times. After the beads had been transferred to a microfuge tube and the supernatant removed, the captured proteins were on-bead digested with trypsin according to standard protocols,²³ and the tryptic peptides were desalted and analyzed by LTQ liquid chromatography and tandem mass spectrometry (LC–MS/MS). Peptides were separated on a 75 μ m (inside diameter) \times 15 cm reverse phase C18 column (Thermo) controlled by an Ultimate 3000 nanoflow HPLC system (Dionex) and eluted using a 55 min gradient from 2 to 55% solvent B (99.9% acetonitrile and 0.1% formic acid) at a flow rate of 0.3 μ L/min, and further introduced into an LTQ-Orbitrap Velos mass spectrometer (Thermo Fisher). The mass

spectrometer was operated in LTQ data-dependent mode, automatically switching between MS and MS/MS. Full scan MS spectra (300–2000 amu) were analyzed in a profile mode with the LTQ analyzer. The seven most intense ions in a scan were selected for collision-induced fragmentation (CID) in the LTQ instrument at a normalized collision energy of 35% with an activation time of 40 ms. The acquired data were analyzed with Proteome Discoverer 1.4 (Thermo Fisher) using the SEQUEST algorithm and a human Uniprot database along with the reversed decoy database. Searches were done using a precursor mass tolerance of 1.8 Da and fragment tolerance of 0.5 Da, and the following dynamic modifications were included: oxidation of methionine, N-terminal acetylation, and carbamidomethylation of cysteine. The results were filtered using normalized XCorr values for different charge states²⁴ and were accepted as valid identifications only if the XCorr values were >1.5, >2.5, >3.75, and >4 for singly, doubly, triply, and quadruply charged peptides, respectively. Moreover, the maximal Δ Cn was 0.15 for peptides. Proteins with a minimum of two peptides detected using the settings given above were considered for the final list of proteins. The proteins were further grouped, where PSMs with only a high degree of confidence were used, and the strict maximal parsimony principle was applied to the protein groups. Normalized spectral counts for each identified serine hydrolase were determined using the commercially available Scaffold version 4.0.7.

Identification of Palmitoyl Protein Thioesterase 1: ABPP–In-Gel Digest–MUDPIT. THP1 monocyte lysate [1 mg/mL protein in 50 mM Tris-HCl (pH 7.4)] was incubated with an activity-based probe (FP-biotin, final concentration of 4 μ M) for 1 h at room temperature followed by removal of excess FP-biotin. To control for nonspecific and noncatalytic labeling of proteins by FP-biotin, a separate equivalent amount of lysate protein was heated for 5 min (95 °C) to denature proteins prior to the addition of FP-biotin. The biotinylated proteins were captured by addition of streptavidin beads (100 μ L) and the beads washed as previously described.¹⁴ Proteins were eluted from the beads by addition of 50 μ L of 2 \times SDS–PAGE loading buffer (reducing) and heating (95 °C for 5 min). After separation of the affinity-enriched proteins by 10% SDS–PAGE, the gel was stained with Coomassie blue (Biosafe, Bio-Rad) for 4 h at room temperature. The gel bands, ranging in size between 31 and 43 kDa, were excised with a razor blade. Proteins were in-gel digested with trypsin according to standard protocols, and the resulting peptides were desalted and analyzed by LTQ LC–MS/MS as described above.

Expression of PPT1 in THP1 Monocytes and Macrophages and Other Cells. Whole-cell lysates [typically prepared in 50 mM Tris-HCl (pH 7.4)] from THP1 monocytes and macrophages, primary murine macrophages, primary human monocytes, or HepG2 cells were separated by SDS–PAGE. Following electrophoretic transfer, PVDF membranes were probed with either rabbit anti-CES1 [1:4000 (v/v)] or mouse anti-PPT1 (1 μ g/mL) in 3% nonfat milk overnight at 4 °C. Membranes were washed followed by incubation with secondary antibodies conjugated to horseradish peroxidase [1:20000 (v/v)]. Following addition of luminol reagent, chemiluminescence was recorded using X-OMAT photographic film (Eastman Kodak Co., Rochester, NY). Increasing amounts of recombinant CES1 and PPT1 (10, 25, 50, and 100 ng) were used on gels as calibrants for semiquantitative immunoblots.

In addition, THP1 monocyte lysate was treated with FP-biotin and biotinylated proteins enriched using streptavidin beads, as described above. After separation of eluted proteins by SDS-PAGE and electrophoretic transfer to a PVDF membrane, the biotinylated proteins were detected using either avidin-horseradish peroxidase or anti-PPT antibodies.

Transduction of shRNA-Containing Lentiviral Particles into THP1 Monocytes. THP1 monocytes were plated into a 12-well plate (5×10^5 cells/well) in complete RPMI medium (RPMI 1640 supplemented with 10% FBS, 0.05 M 2-mercaptoethanol, and 0.05 mg/mL gentamicin) containing 8 μ g/mL Polybrene. Two wells were inoculated with control lentiviral particles [0.1 MOI (multiplicity of infection), scrambled shRNA, Santa Cruz Biotechnology, sc-108080] and two wells inoculated with CES1 shRNA lentiviral particles (0.1 MOI, CES1 shRNA, Santa Cruz Biotechnology, sc-62096-V). The lentivirus-treated cells were cultured overnight; the medium was subsequently replaced with complete RPMI medium (without Polybrene), and cells were incubated for an additional 24 h. The cells were then split 1:2 and incubated for an additional 24–48 h. To select stable clones of THP1 cells expressing shRNA, the culture medium was replaced with complete RPMI medium containing 5 μ g/mL puromycin dihydrochloride. The medium was replaced with fresh puromycin-containing medium every 3–4 days for a 3 week period. Only puromycin-resistant cells were used for subsequent experiments. Knockdown of CES1 in the THP1 cells was verified by the pNPV activity assay and CES1 immunoblot analysis. Lysates of parental THP1 cells (control) and CES1-deficient THP1 cells were used to compare 2-AG hydrolysis rates.

Intact monocytes (both control and CES1-deficient; 1.2×10^6 cells/well) were treated with ionomycin (3 μ M) in serum-free RPMI medium (2 mL) to stimulate *in situ* biosynthesis of 2-AG; the levels of 2-AG released into the culture medium were determined after 1 h, as described previously.¹⁰

Preparation of Recombinant Human PPT1 from a CHO Cell Line. CHO-hPPT1 cells²⁵ were cultured in nucleoside-deficient minimal essential medium containing 30 μ M methotrexate, 10% dialyzed FBS, 100 units/mL penicillin, 100 μ g/mL streptomycin, and 0.25 μ g/mL amphotericin B. For the production of recombinant PPT1 protein, confluent adherent CHO-hPPT1 cells were split 1:2 and grown in F-12 medium (Invitrogen) supplemented with 10% regular FBS until they were confluent. The cells were washed with serum-free medium three times and subsequently cultured in serum-free Hyclone medium (CDM4CHO, SH30557) for 12–14 days, with medium collected (and stored 4 °C) every 2 days, and the cells were replenished with fresh medium. Typically, eight 100 mm dishes each containing 5 mL of medium were used. The pooled media were collected by centrifugation at 400g (4 °C), filtered through a 0.2 μ m filter unit to remove debris and floating cells, and concentrated approximately 40-fold using a stirred cell equipped with a YM-10 membrane (Millipore) at 4 °C. The concentrated protein was subsequently exchanged into 50 mM Tris-HCl (pH 7.4) buffer containing 0.1 mM EDTA and 20% (v/v) glycerol by repeated rounds of concentration and dilution through a YM-3 centrifugal filter. The protein concentration was measured, and aliquots were snap-frozen in liquid nitrogen and stored at –80 °C. Protein purity and identity were verified by Coomassie blue staining of SDS-PAGE gels and immunoblot analysis using a polyclonal mouse anti-PPT1 antibody. Using 4-MUBO as a substrate (final

concentration of 75 μ M), the specific activity for the recombinant human PPT1 protein was determined to be 336 nmol min^{–1} (mg of protein)^{–1}, which is ~10-fold higher than the specific activity of recombinant human CES1 using the same substrate.¹⁴ In terms of yield, ~260 mL of conditioned serum-free medium from CHO-hPPT1 cells yielded ~64 mg of crude PPT1 protein.

Hydrolysis of 2-AG and PG-Gs by Recombinant Human PPT1 or CES1. Hydrolysis reactions with recombinant protein (5 μ g of PPT1 or 0.2 μ g of CES1 per reaction) were performed in 50 mM Tris-HCl (pH 7.4) buffer supplemented with 0.01% (w/v) fatty acid-free bovine serum albumin (BSA) and lipid glyceryl substrate varying from 0 to 200 μ M (for PG-Gs) and from 0 to 400 μ M (for 2-AG) in a total reaction volume of 100 μ L. After preincubation of the buffer and substrate for 5 min at 37 °C, reactions were initiated by addition of recombinant enzyme or buffer alone (non-enzymatic control). Reactions were quenched after 30 min with an equal volume of cold acetonitrile containing internal standards, 8-iso-PGF_{2 α} -d₄ (140 pmol for the PG-G hydrolysis reaction) or AA-d₈ (500 pmol for the 2-AG hydrolysis reaction). Quenched reaction mixtures were placed on ice for 15 min and then centrifuged at 16000g (4 °C for 5 min) prior to supernatants being transferred into HPLC vials. Supernatants were analyzed for hydrolysis product PGE₂, PGF_{2 α} , or AA by LC-MS/MS and quantification using the stable isotope procedure. Kinetic parameters of the hydrolysis reactions (k_{cat} , K_m , and k_{cat}/K_m) were determined by performing nonlinear regression analysis using the Michaelis–Menten equation with Sigma Plot version 8.02.

Residual 2-AG Hydrolysis Activity of Recombinant Human PPT1 following JZL184, PO, and HDSF Treatments: Comparison to Recombinant Human CES1. Inhibition reactions were performed in 50 mM Tris-HCl (pH 7.4) buffer containing 0.01% (w/v) fatty acid-free BSA, 10 μ M 2-AG, recombinant enzyme, and various amounts of inhibitor in a total volume of 100 μ L. Recombinant PPT1 enzyme (5 μ g) was added to reaction mixtures containing 1 or 10 μ M JZL184, 10 or 100 μ M PO, and 200 μ M HDSF. After preincubation (30 min at 37 °C) of the enzyme and inhibitors, hydrolytic reactions were initiated by addition of 2-AG (final concentration of 10 μ M). After 30 min, reactions were quenched with an equal volume of acetonitrile containing internal standard (AA-d₈, 500 pmol), and mixtures were placed on ice and centrifuged at 16000g for 5 min (4 °C). Supernatants were analyzed for AA by LC-MS/MS.

Treatment of THP1 Macrophages with PO and HDSF, Followed by Addition of 2-AG. THP1 monocytes (3×10^6 cells) were seeded into a six-well plate in complete growth medium and differentiated into macrophages by the addition of PMA (70 nM) for 48–72 h. After cell differentiation, the culture medium was removed and the cells were washed with Hank's buffer. Cells were then overlaid with serum-free culture medium containing PO (10 μ M), HDSF (200 μ M), or vehicle [0.1% (v/v) ethanol] and incubated for 30 min. 2-AG was then directly added to the culture medium (final concentration of 10 μ M) and incubation continued for an additional 60 min. The cells were collected, and the culture medium was removed for analysis. The cells were washed three times with ice-cold PBS and resuspended in 50 mM Tris-HCl (pH 7.4) buffer, and lysates were prepared by sonication. The PPT1 activity of the lysates was determined using either pNPV or 4-MUBO as a substrate²⁶ to verify inhibition by PO and HDSF. The culture

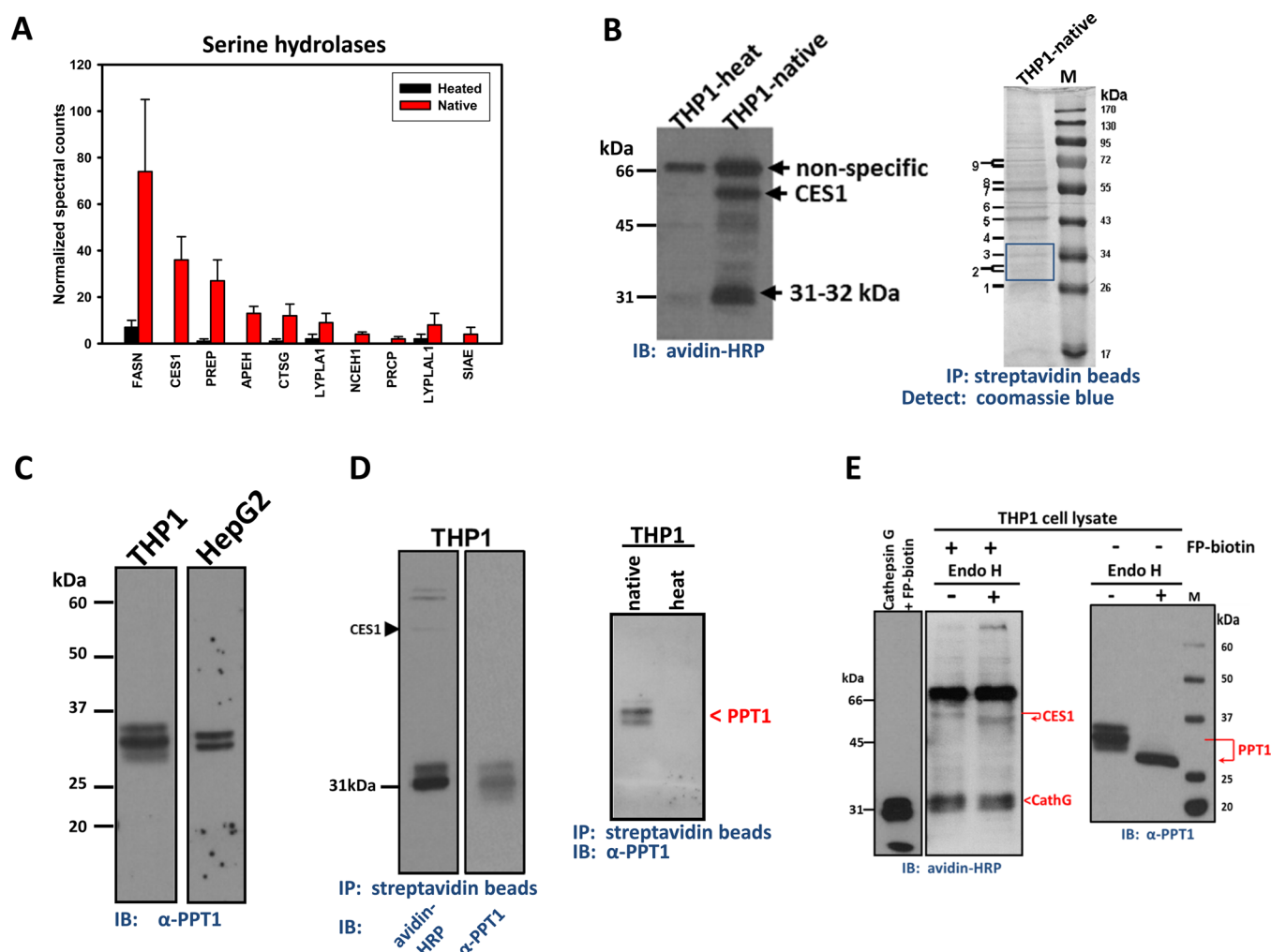


Figure 1. Identification of serine hydrolases, including PPT1 in THP1 cells. (A) ABPP–MUDPIT of serine hydrolases in THP1 monocytes. The relative amounts of each serine hydrolase were semiquantified by spectral counting of tryptic peptides. Heated or Native indicates the cell lysate was heat denatured (90 °C for 5 min) or not, respectively, prior to treatment with FP-biotin (8 μ M for 1 h at room temperature). Data represent means \pm the standard error of the mean of duplicate analyses. The full list of identified serine hydrolases (including abbreviations and molecular masses) is given in Table 1 of the Supporting Information. (B) Serine hydrolase activity profile of THP1 monocytes determined using FP-biotin (left). THP1-heat or THP1-native indicates that lysates were heated or not heated, respectively, prior to reaction with FP-biotin. The THP1 monocyte lysate was treated with FP-biotin followed by enrichment of labeled proteins using streptavidin beads (right). Captured proteins were separated by SDS–PAGE and detected with Coomassie blue. Abbreviations: M, molecular weight marker; IP, immunoprecipitation; IB, immunoblot. (C) PPT1 immunoblot of whole THP1 monocyte and HepG2 cell lysates separated by SDS–PAGE. (D) FP-biotin-treated THP1 cell lysates were enriched on streptavidin beads and the captured proteins separated by SDS–PAGE (left). PVDF membranes were probed with either avidin–horseradish peroxidase (HRP) or anti-PPT1 antibodies. Note that three bands are detected at \sim 31 kDa in the anti-PPT1 blot, whereas two bands are detected in the avidin-HRP blot. This indicates that detection of PPT1 with antibodies is more sensitive than avidin blotting. Native and heat indicate that FP-biotin reacts only with active PPT1 in the THP1 cell lysate prior to pull down on streptavidin beads (right); PPT1 was detected after SDS–PAGE by anti-PPT1 antibodies. (E) THP1 monocyte lysates pretreated with FP-biotin (left) or not pretreated (right) were subsequently treated overnight with or without endoglycosidase H and the resulting samples separated by SDS–PAGE, followed by avidin-HRP (left) or a PPT1 immunoblot (right). Also shown (far left) is pure cathepsin G treated with FP-biotin (8 μ M for 1 h at room temperature) prior to SDS–PAGE and avidin blotting.

medium was spiked with internal standard (AA- d_8 , 500 pmol) and extracted with 3 volumes of ethyl acetate containing 0.1% acetic acid. The ethyl acetate layer was recovered and evaporated to dryness under nitrogen. The residues were redissolved in 100 μ L of an acetonitrile/water mixture [1:1 (v/v)], filtered through a microfuge filter unit (0.22 μ m), and transferred to LC vials for LC–MS/MS analysis.

2-AG Hydrolysis by Immunodepleted THP1 Monocyte Lysates. THP1 monocyte lysate (1 mg of protein/mL) was solubilized in 50 mM Tris-HCl (pH 7.4) buffer containing 10% (v/v) fatty acid-free BSA (mixed on a rotator for 1 h at 4 °C) and then incubated overnight at 4 °C with preimmune IgG

antibodies (nonspecific control) or anti-PPT1 IgG antibodies. The mixtures were subsequently transferred to protein A–agarose beads, which had been prewashed three times with IP wash buffer [50 mM Tris-HCl (pH 7.4) supplemented with 300 mM NaCl, 5 mM EDTA, and 0.1% (v/v) Triton X-100], and incubated for 4 h on a rotator (at 4 °C). The beads were pelleted in a microcentrifuge, and the resulting immunodepleted supernatants were used for immunoblot analysis and hydrolysis reactions. For 2-AG hydrolysis reactions, triplicate reactions were performed in 50 mM Tris-HCl (pH 7.4) buffer containing 2-AG (final concentration of 10 μ M) in a total reaction volume of 50 μ L. After preincubation of the buffer and

substrate for 5 min at 37 °C, reactions were initiated by addition of 25 µg of control or immunodepleted THP1 cell lysates. Reactions were quenched after a 30 min incubation with an equal volume of acetonitrile containing internal standard AA-*d*₈ (500 pmol) and placed on ice for 15 min. Samples were centrifuged at 16000g for 5 min (4 °C) to remove precipitated protein prior to supernatants being transferred into HPLC vials. The AA content of the supernatant was determined by LC–MS/MS.

LC–MS/MS Analytical Procedures. Analysis of products obtained from recombinant enzyme-catalyzed reactions and THP1 cell/medium extracts was performed on a Thermo UPLC–MS/MS system (Thermo Fisher Scientific, San Jose, CA). Samples (10 µL) were injected into an Acquity UPLC BEH C18 column (2.1 mm × 100 mm, 1.7 µm) equipped with a VanGuard precolumn (2.1 mm × 5 mm, 1.7 µm). For arachidonic acid and prostaglandins (AA, AA-*d*₈, PGE₂, PGF_{2α}, and 8-iso-PGF_{2α}-*d*₄), the mobile phases used were a blend of solvent A [0.1% (v/v) acetic acid in water] and solvent B [0.1% (v/v) acetic acid in acetonitrile], and the gradient program was as follows: 20% A and 80% B at 0 min, 20% A and 80% B at 0.25 min, 0% A and 100% B at 2.0 min, 0% A and 100% B at 3.0 min, 20% A and 80% B at 3.5 min, and 20% A and 80% B at 5.0 min. For neutral glyceryl ester analytes (2-AG and 2-AG-*d*₈), the mobile phases were a blend of solvent A (2 mM ammonium acetate and 0.1% acetic acid in water) and solvent B (2 mM ammonium acetate and 0.1% acetic acid in methanol), and the gradient program was as follows: 95% A and 5% B at 0 min, 95% A and 5% B at 0.5 min, 5% A and 95% B at 5 min, 5% A and 95% B at 6 min, 95% A and 5% B at 7 min, and 95% A and 5% B at 8 min. The flow rate was 0.4 mL/min and the column eluate directed into the mass spectrometer using heated electrospray ionization in either negative or positive ion mode. Single-reaction monitoring (SRM) of analytes was as follows: AA, [M – H][–] *m/z* 303.1 > 259.4; AA-*d*₈, [M – H][–] *m/z* 311.2 > 267.2; PGE₂, [M – H][–] *m/z* 351.2 > 271.2; PGF_{2α}, [M – H][–] *m/z* 353.2 > 193.1; 8-iso-PGF_{2α}-*d*₄, [M – H][–] *m/z* 357.2 > 197.1; 2AG, [M + NH₄]⁺ *m/z* 396.3 > 287.3; and 2AG-*d*₈, [M + NH₄]⁺ *m/z* 404.3 > 293.5. Scan times were 0.2 s per SRM, and the scan width was *m/z* 0.01. Collision energies and the tube lens voltage were optimized using autotune software for each analyte by postcolumn infusion of the individual compounds into a 50% A/50% B blend of the mobile phase being pumped at a flow rate of 0.4 mL/min. Internal standards AA-*d*₈, 8-iso-PGF_{2α}-*d*₄, and 2-AG-*d*₈ were used for quantification. Calibration standards containing each analyte were routinely prepared in serum-free RPMI culture medium at four different concentrations (1, 0.1, 0.01, and 0.001 µM). The spiked culture medium was fortified with internal standards (7 pmol of 8-iso-PGF_{2α}-*d*₄ and 500 pmol of AA-*d*₈) and extracted with ethyl acetate, as described above.

RESULTS

Identification of Cathepsin G and PPT1 in THP1 Monocytes and Macrophages. On the basis of chemical proteomic–LC–MS/MS and immunoblotting analyses (Figure 1), we identified several serine hydrolases in human THP1 cells, including cathepsin G (CTSG) and palmitoyl protein thioesterase 1 (PPT1). Ten catalytically active serine hydrolases were identified by ABPP–MUDPIT (Figure 1A and Table 1 of the Supporting Information). One of the 10, the serine protease cathepsin G, has a molecular mass similar to that of the unknown protein-derived signals at ~31–32 kDa in activity

gels (Figure 1B, left, and ref 10). In addition, subsequent to FP-biotin treatment of THP1 cell lysate, streptavidin bead-enriched proteins were subjected to electrophoresis, and Coomassie-stained bands indicated by a rectangle [~30–34 kDa (Figure 1B, right)] were digested with trypsin. Several proteins were identified by LC–MS/MS analysis of the tryptic peptides using the SEQUEST search algorithm, including the serine hydrolase PPT1 (Figure 1 of the Supporting Information). Interestingly, PPT1 was not identified by the ABPP–MUDPIT approach (Figure 1A), but only after trypsin digestion of gel bands in the 30–34 kDa region. Thus, the proteomic analyses taken as a whole suggested that PPT1 and cathepsin G were both candidate enzymes that accounted for the 31–32 kDa signals on activity gels. It is noteworthy that the validated 2-AG hydrolytic enzymes MAGL, FAAH, ABHD6, and ABHD12 were not detected by either ABPP–MUDPIT or in-gel digestion and LC–MS/MS analysis of peptides.

On the basis of Western blot analysis, PPT1 was abundantly expressed in THP1 cells (Figure 1C). Immunoblots of whole THP1 monocyte lysates following SDS–PAGE revealed three separate immunoreactive bands that reacted with anti-PPT1 antibodies, while a doublet band pattern was observed in the HepG2 cell line. In addition, cellular PPT1 protein was covalently labeled with the chemoproteomic probe FP-biotin, affinity captured on streptavidin beads, and subsequently detected by immunoblotting using either avidin–horseradish peroxidase or anti-PPT1 antibodies following separation of proteins by SDS–PAGE (Figure 1D). Multiple protein forms detected by PPT1 antibodies suggested that PPT1 was glycosylated, and its heat-sensitive reactivity toward FP-biotin was consistent with it being a member of the serine hydrolase family (Figure 1D).

It was subsequently determined that pure recombinant human PPT1 was not very reactive toward FP-biotin. For instance, pretreatment of recombinant PPT1 with 10 µM FP-biotin inhibited just 18% of PPT1's hydrolytic activity toward the substrate 4-MUBO. Moreover, FP-biotin-treated recombinant PPT1 protein was weakly detected by gel-based ABPP (data not shown). Meanwhile, ~30% of the 2-AG hydrolytic activity in THP1 whole-cell lysate was insensitive to pretreatment with FP-biotin (Figure 2 of the Supporting Information). Together, these findings were consistent with extensive data obtained on mouse brain serine hydrolases indicating that PPT1, although expressed at high levels in the brain,²⁷ was not strongly labeled by FP activity-based probes,²⁸ although a small amount of PPT1 was detected in conditioned medium obtained from the mouse macrophage RAW264.7 cell line.²⁸ In contrast, we found that cathepsin G was readily labeled by FP-biotin and detected by gel-based ABPP (Figure 1E, left). This result was consistent with the large amounts of cathepsin G detected in mouse peritoneal macrophages by ABPP–MUDPIT.²⁹ Therefore, because PPT1 and cathepsin G were detected in THP1 cells by proteomic methods, it is likely that both proteins comigrate on SDS–PAGE gels and that the strongly labeled cathepsin G masked the weaker PPT1 signals on activity gels (Figure 1B, left). Supporting evidence of this includes the following. (i) Endoglycosidase H treatment of the FP-biotin-treated THP1 cell lysate did not alter the migration rate of the 31–32 kDa signals on an activity gel, whereas it did alter the migration behavior of the glycosylated proteins CES1 and PPT1 (Figure 1E). (ii) Although the sulfonyl fluoride inhibitor HDSF inhibits PPT1 (*vide infra*), it did not diminish the magnitude of the 31–32 kDa signals on activity gels (Figure 3A

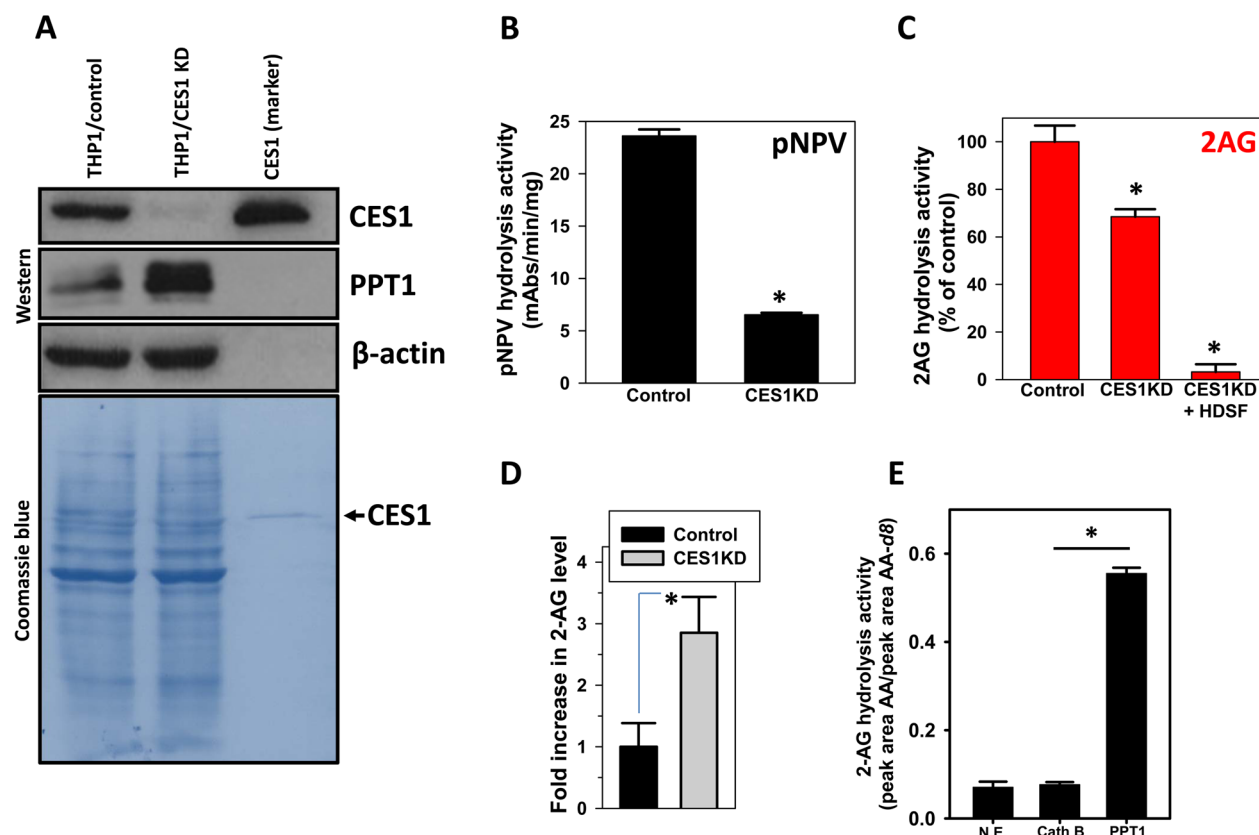


Figure 2. CES1 knockdown in THP1 cells using lentiviral shRNA. (A) Immunoblot analysis for CES1 and PPT1 in control THP1 monocytes (THP1/control) and CES1-deficient THP1 monocytes (THP1/CES1 KD). Coomassie blue detection of proteins on a PVDF membrane and β -actin immunoblot verified equal protein loading (50 μ g per lane). Recombinant CES1 protein was used as a molecular weight marker and positive control. pNPV hydrolytic activity (B) and 2-AG hydrolytic activity (C) of whole-cell lysates obtained from THP1 monocytes (control) and CES1-deficient THP1 monocytes (CES1 KD). Inhibition of the remaining 2-AG hydrolytic activity in CES1-deficient THP1 monocytes (CES1KD +HDSF) was achieved by incubating the lysate with 200 μ M HDSF for 30 min prior to adding 2-AG. (D) Intact control and CES1-deficient THP1 monocytes were treated with ionomycin (3 μ M), followed by determination of 2-AG levels in the culture supernatant after a 60 min pNPV hydrolysis assay of cell lysates confirmed knockdown of CES1 protein (data not shown). (E) 2-AG hydrolytic activity of pure cathepsin G and PPT1 proteins. Abbreviations: N.E., nonenzymatic hydrolysis; Cath G, cathepsin G. Data in each panel represent the means \pm the standard deviation of three independent experiments. * p < 0.05 (Student's t test). mAbs denotes milliabsorbance units.

of the Supporting Information), nor did it inhibit pure cathepsin G activity at 200 μ M (Figure 3B of the Supporting Information). Further, the potent MAGL inhibitor JZL184 and the organophosphate poison paraoxon (PO) also had no effect on this enzyme activity (Figure 3A of the Supporting Information). On the other hand, the general serine hydrolase inhibitor, MAFP, reduced the intensity of the 31–32 kDa signals in the THP1 cell lysate (Figure 3C of the Supporting Information) and pure cathepsin G (Figure 3D of the Supporting Information). MAFP also blocked pure recombinant PPT1 hydrolytic activity toward 4-MUBO (data not shown), indicating it could inhibit both cathepsin G and PPT1.

Treatment of THP1 monocyte lysate with endoglycosidase H, which recognizes and hydrolyzes N-type glycans attached to asparagine residues, caused three PPT1 immunoreactive bands with M_r values of 31, 33, and 35 kDa to collapse into a single, faster-migrating immunoreactive band with an M_r of ~29 kDa (Figure 1E). This result is consistent with the fact that human PPT1 has three asparagine-linked glycosylation sites at amino acid positions 197, 212, and 232.³⁰ The rank order of abundance for each glycosylated PPT1 form was as follows: diglycosylated > triglycosylated > monoglycosylated.

Knockdown of CES1 Expression in THP1 Monocytes. Previous findings that suggested CES1 was a 2-AG hydrolytic

enzyme¹⁰ were verified by knocking down CES1 expression in THP1 cells (Figure 2). The level of CES1 protein expression was markedly reduced in THP1 cells using a lentiviral CES1 shRNA system, as determined by both immunoblot analysis (Figure 2A) and esterase activity (Figure 2B) of control and CES1-deficient cells. Interestingly, PPT1 protein expression appeared to be slightly enhanced in the CES1-deficient cells. Hydrolysis of 2-AG by cell lysates obtained from control and CES1-deficient (CES1 KD) THP1 monocytes demonstrated that CES1 knockdown reduced 2-AG hydrolytic activity by 32% relative to the control (Figure 2C). Further, treatment of CES1-deficient lysate with 200 μ M HDSF inhibited nearly all the remaining 2-AG hydrolytic activity (Figure 2C; 97% reduction compared to control). Moreover, stimulation of living CES1-deficient THP1 monocytes with ionomycin, which stimulates biosynthesis of 2-AG, caused 2-AG levels to be elevated nearly 3-fold compared to those of control cells (Figure 2D). Further *in vivo* relevance for CES1 in 2-AG metabolism was evident from the fact that THP1 macrophages were activated by being exposed to lipopolysaccharide (to induce COX-2), followed by addition of exogenous 2-AG in the presence or absence of benzil, a CES1 inhibitor³¹ (Figure 4A of the Supporting Information). Upon 2-AG hydrolysis, AA is oxygenated by COX-2 to yield prostaglandins in specific tissues.^{32,33} Crucial to

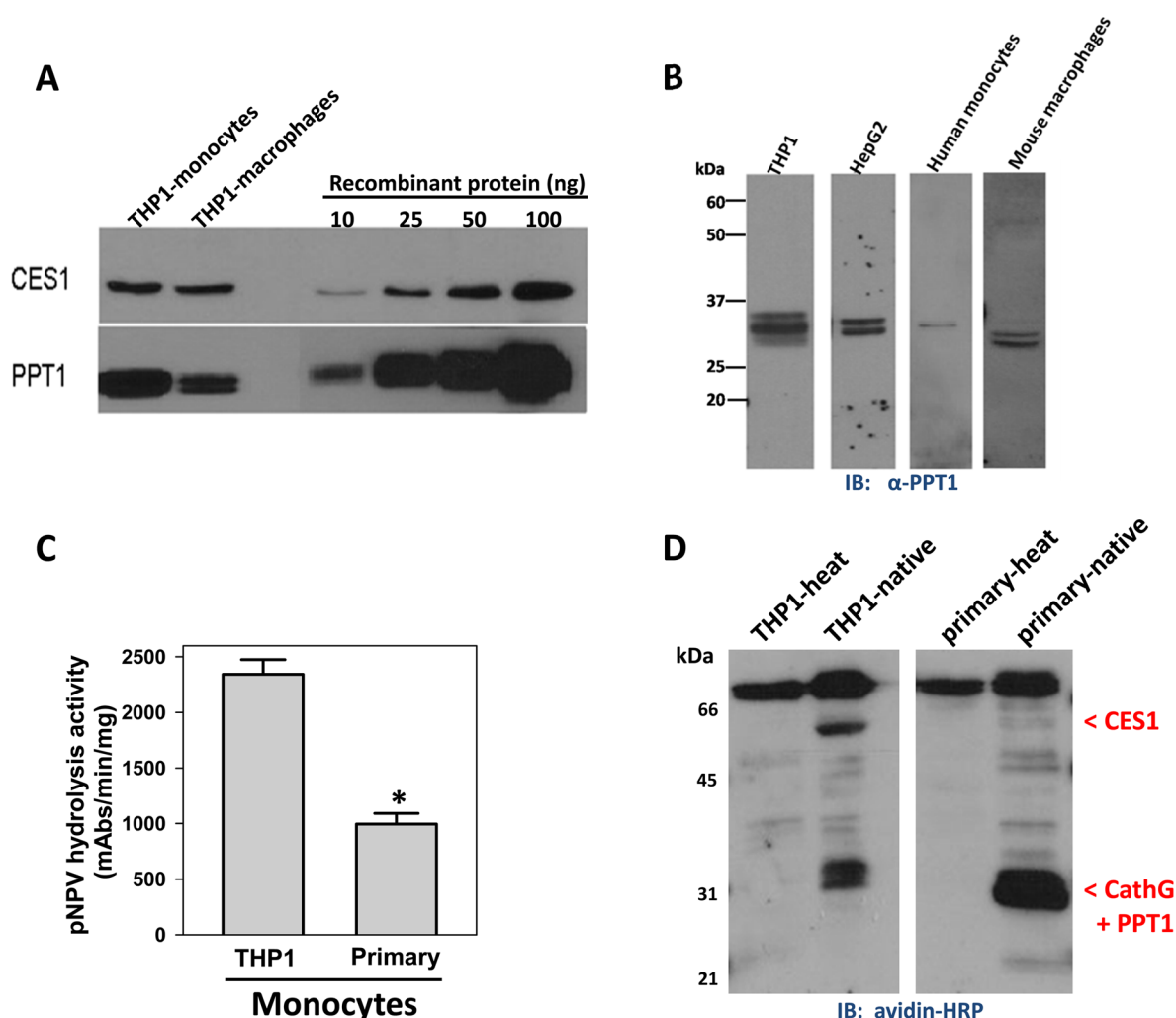


Figure 3. Expression levels of PPT1 in monocytes and macrophages. (A) Semiquantification of PPT1 and CES1 in THP1 monocytes and macrophages by immunoblot analysis. (B) PPT1 immunoblot of cell lysate proteins obtained from THP1 monocytes, HepG2, human primary monocytes, and mouse primary macrophages. The HepG2 blot in Figure 1C is reproduced here for the purpose of comparison only. Note that we verified that anti-PPT1 does not cross-react with pure human cathepsin G (data not shown). (C) Esterase activity of THP1 monocytes and primary human monocytes determined using pNPV. Data are means \pm the standard deviation of three independent experiments. * $p < 0.05$ (Student's t test). (D) Serine hydrolase activity profile of THP1 monocytes and primary human monocytes determined using FP-biotin. Locations of CES1, PPT1, and cathepsin G are indicated.

this mechanism is the regulation of 2-AG hydrolysis. Thus, we speculated that inhibition of CES1-mediated 2-AG hydrolysis in intact macrophages would partially reduce the size of the pool of precursor AA available to COX-2. In line with this, pretreatment with benzil significantly reduced the levels of PGF_{2 α} and PGE₂ synthesized by macrophages (Figure 4A of the Supporting Information). Inhibition of the 2-AG biosynthetic enzyme, DAGL β , by RHC-80267 also resulted in decreased levels of prostaglandins following stimulation of cellular 2-AG biosynthesis by ionomycin (Figure 4B of the Supporting Information), which is consistent with the partially reduced 2-AG and prostaglandin production that was observed following DAGL β blockade in murine peritoneal macrophages by Hsu et al.²⁹

To examine the possibility that cathepsin G and PPT1 also contribute to 2-AG hydrolytic activity, we used pure cathepsin G and PPT1 proteins and determined whether they hydrolyzed 2-AG *in vitro*. As indicated in Figure 2E, PPT1 catalyzed the hydrolysis of 2-AG but cathepsin G did not. In light of the fact that MAGL, FAAH, ABHD6, and ABHD12 were either

undetectable or expressed at very low levels in THP1 cells, we followed up on the possibility that PPT1 contributed to the 2-AG hydrolysis activity for which CES1 did not account.

Expression Levels of PPT1 in Human THP1 Monocytes and Macrophages and Other Cells. First, we determined the amount of PPT1 expressed in THP1 cells to compare it with levels of CES1. Semiquantitative immunoblotting analysis performed on THP1 whole-cell lysates indicated that PPT1 was abundant in both THP1 monocytes and macrophages, with expression levels of 75 ± 3 and 28 ± 8 pmol/mg of lysate protein, respectively (Figure 3A). On a molar basis, PPT1 was more abundant than CES1 in THP1 monocytes and macrophages; PPT1 levels were 3- and 1.5-fold greater than CES1 levels, respectively. In addition, the amount of PPT1 in THP1 macrophages was estimated to be ~ 34 -fold greater than the amount of the canonical 2-AG hydrolytic enzyme, MAGL, based on our previously published data.¹⁰

In addition to THP1 cells, we determined that PPT1 was expressed in HepG2, human primary monocytes, and mouse peritoneal macrophages (Figure 3B), indicating PPT1 is

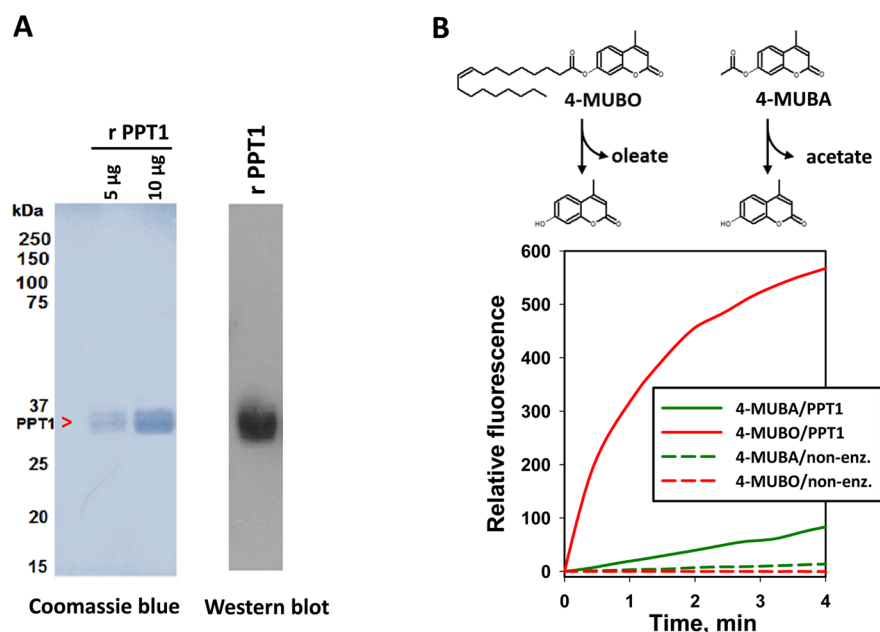


Figure 4. Production of recombinant PPT1 in stably overexpressing CHO cells. (A) Coomassie blue staining (left) and immunoblot analysis (right) of recombinant (r) PPT1 protein produced by CHO-hPPT1 cells. (B) Activity progress curves for hydrolysis of 4-MUBO and 4-MUBA by recombinant PPT1. Data represent the mean fluorescence obtained from at least three independent reactions for each condition. The variation (standard deviation) in the activity progress curves for each condition was <10%.

distributed in multiple cell types. Another notable finding was that CES1 expression was less abundant in primary human monocytes than in THP1 cells on the basis of esterase activity (Figure 3C), gel-based ABPP (Figure 3D), and immunoblot analysis (data not shown). Furthermore, gel-based ABPP indicated the 31–32 kDa activity signals, which are likely caused by comigration of cathepsin G and PPT1, were clearly observable in both primary human monocytes and THP1 cells (Figure 3D).

Expression and Isolation of Recombinant Human PPT1. Having determined that PPT1 is abundantly expressed in THP1 cells, we next examined the biochemical activities of this serine lipase in more detail using recombinant human PPT1 protein. The Coomassie blue-stained gel and Western blot of the PPT1 protein produced by CHO-hPPT1 cells showed a single diffuse band around 34 kDa (Figure 4A), which is consistent with the protein being glycosylated in a heterogeneous manner. On the basis of the Coomassie blue-stained gel (Figure 4A), the recombinant PPT1 protein preparation was estimated to be >90% pure. Furthermore, mass spectrometric analysis of tryptic peptides derived from the recombinant protein confirmed its identity was PPT1 and indicated it was not contaminated by another serine hydrolase such as MAGL (data not shown). Recombinant PPT1 could hydrolyze both small acyl ester substrates (4-MUBA) and fatty acyl ester substrates (4-MUBO) (Figure 4B); however, it was more effective (28-fold) at hydrolyzing substrates with a fatty acyl moiety, such as the oleoyl group in 4-MUBO, compared to acetyl-containing substrates such as 4-MUBA. The kinetic parameters for 4-MUBO hydrolysis by PPT1 (assuming a molecular mass of 34 kDa) were as follows: $k_{\text{cat}} = 2.79 \pm 0.05 \text{ min}^{-1}$, and $K_m = 21.8 \pm 0.4 \text{ } \mu\text{M}$ (mean \pm range, $n = 2$ determinations). These results demonstrated that PPT1, although termed a thioesterase, also acts as an esterase and lipase.

Hydrolysis of 2-AG and PG-Gs by Recombinant Human PPT1: Comparison to That of CES1.

Because recombinant human PPT1 could hydrolyze the ester-containing 2-AG (Figure 2E), we next characterized the kinetics of the reaction (Figure 5A) and compared the catalytic efficiency of PPT1 to that of CES1 (Figure 5A, inset, and Table 1). In addition to 2-AG, PPT1 also hydrolyzed $\text{PGE}_2\text{-G}$ and $\text{PGF}_{2\alpha}\text{-G}$ to their respective free prostaglandins (Figure 5B). The extent of 2-AG and PG-G hydrolysis by recombinant PPT1 was protein concentration-dependent (data not shown), time-dependent (2-AG hydrolysis shown in Figure 5C), and concentration-dependent (Figure 5A,B). Steady-state Michaelis–Menten kinetic parameters for 2-AG hydrolysis reactions catalyzed by human PPT1 and CES1 are reported in Table 1. The turnover number (k_{cat}) for PPT1 is 246-fold lower than that for CES1, whereas the catalytic efficiency (k_{cat}/K_m) for PPT1 was only 13-fold lower than that for CES1. K_m values for the substrate–enzyme pairs differed by 20-fold; however, because deacylation of the acyl–enzyme intermediate is usually rate-limiting for the hydrolysis of esters (i.e., $k_2 \gg k_3$),³⁴ K_m is a complex function of individual rate constants and can be difficult to interpret with respect to substrate affinity.³⁴ In addition, the k_{cat}/K_m value for PPT1-catalyzed hydrolysis of 2-AG ($0.093 \text{ min}^{-1} \text{ } \mu\text{M}^{-1}$) was lower than the comparable parameters previously reported for rat and human MAGLs (22- and 8-fold, respectively)³⁵ but similar to the catalytic efficiency of 4-MUBO hydrolysis by PPT1 ($0.13 \text{ min}^{-1} \text{ } \mu\text{M}^{-1}$), giving confidence in its estimate. Thus, on the basis of its Michaelis constant and turnover number, the intrinsic 2-AG hydrolytic activity of PPT1 appears to be maximal at physiological concentrations of 2-AG ($\sim 1\text{--}10 \text{ } \mu\text{M}$).

Prostaglandin glyceryl esters, e.g., $\text{PGE}_2\text{-G}$ and $\text{PGF}_{2\alpha}\text{-G}$, are formed by COX-mediated oxygenation of 2-AG and are prostaglandins that retain the esterified glycerol moiety.¹⁵ Recombinant PPT1 could hydrolyze both $\text{PGE}_2\text{-G}$ and $\text{PGF}_{2\alpha}\text{-G}$, and analysis of substrate concentration–velocity plots

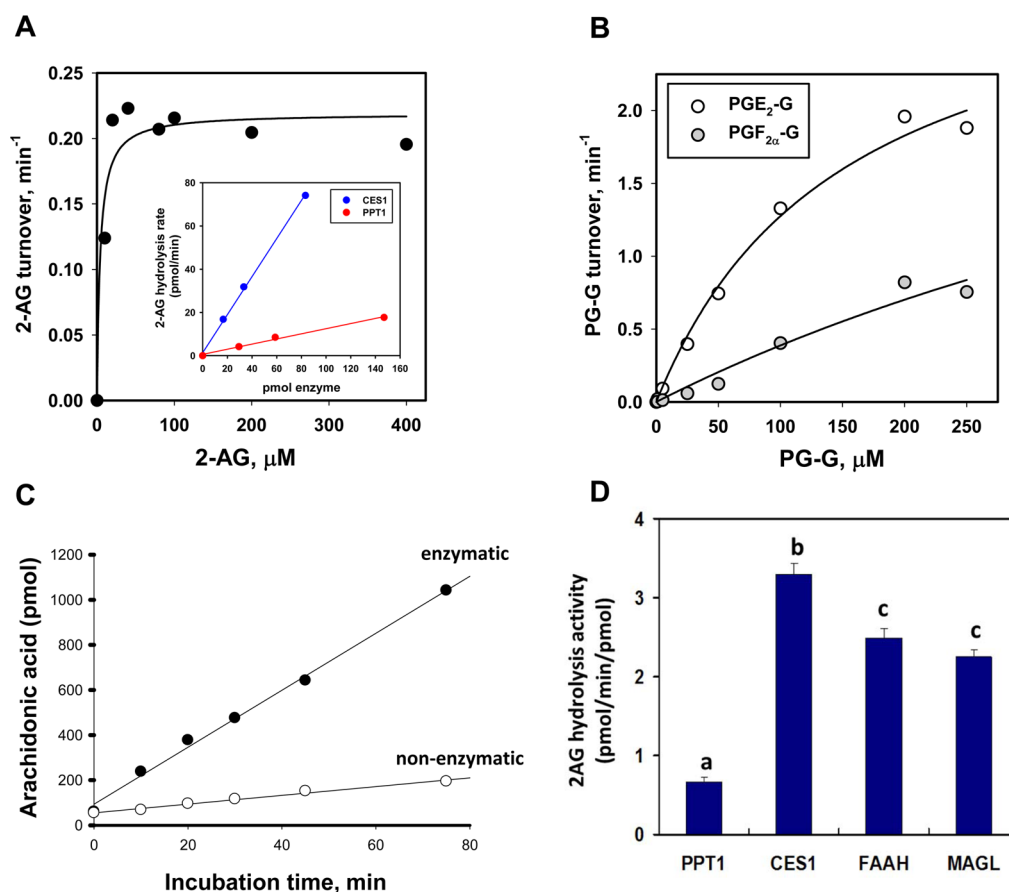


Figure 5. Rates of PPT1-catalyzed hydrolysis of 2-AG and PG-Gs. Substrate concentration vs velocity plots for recombinant PPT1-catalyzed hydrolysis of 2-AG (A) and $\text{PGF}_{2\alpha}\text{-G}$ and $\text{PGE}_2\text{-G}$ (B). Data are representative of at least three independent experiments. The inset in panel A shows the 2-AG hydrolysis rate (final 2-AG concentration of 10 μM) as a function of the amount of either CES1 or PPT1. The slopes for the two lines differ by 7.4-fold. (C) Time course of AA formation when 2-AG (10 μM) was incubated in the presence (enzymatic) or absence (nonenzymatic) of PPT1. (D) Comparison of specific activities for enzymes that hydrolyze 10 μM 2-AG [30 min at 37 $^{\circ}\text{C}$; reaction buffer of 50 mM Tris-HCl (pH 7.4)]. Data represent means \pm the standard deviation of duplicate reactions. Different lowercase alphabetical letters indicate statistical differences between groups ($p < 0.05$, one-way ANOVA and Tukey's test). Data for FAAH and MAGL are from ref 10.

Table 1. Steady-State Kinetic Parameters for the Hydrolysis of 2-AG and PG-Gs by Recombinant Human PPT1 and CES1^a

substrate	k_{cat} (min^{-1})	K_{m} (μM)	$k_{\text{cat}}/K_{\text{m}}$ ($\text{min}^{-1}\mu\text{M}^{-1}$)
PPT1			
2-AG	0.24 ± 0.02	2.5 ± 4.0	0.093 ± 0.002
$\text{PGF}_{2\alpha}\text{-G}$	3.7 ± 0.04	845 ± 0.0	0.0043 ± 0.0004
$\text{PGE}_2\text{-G}$	3.2 ± 0.0	152 ± 0.0	0.021 ± 0.003
CES1			
2-AG	59 ± 4.0	49 ± 11	1.2 ± 0.0
$\text{PGF}_{2\alpha}\text{-G}$	29 ± 3.5	93 ± 43	0.49 ± 0.18
$\text{PGE}_2\text{-G}$	90 ± 16	250 ± 60	0.37 ± 0.05

^aParameters for PPT1 and CES1 are averages \pm the standard deviation of three independent experiments. Kinetic parameters for CES1 are from ref 10.

yielded the Michaelis–Menten parameters for PPT1- and CES1-mediated PG-G hydrolysis reactions reported in Table 1. As judged by $k_{\text{cat}}/K_{\text{m}}$ values, rates of hydrolysis of $\text{PGE}_2\text{-G}$ and $\text{PGF}_{2\alpha}\text{-G}$ by CES1 were not significantly different. On the other hand, $\text{PGE}_2\text{-G}$ was hydrolyzed 5 times faster than $\text{PGF}_{2\alpha}\text{-G}$ by PPT1. When CES1 and PPT1 enzymes are compared, $\text{PGE}_2\text{-G}$

and $\text{PGF}_{2\alpha}\text{-G}$ were hydrolyzed 17 and 114 times faster by CES1 than by PPT1, respectively (Table 1).

The enzymes MAGL, FAAH, CES1, and CES2 have been previously reported to hydrolyze 2-AG and PG-Gs,^{10,35} but this is the first time that these lipid mediators are reported to be substrates for PPT1. We next compared recombinant forms of human MAGL, FAAH, CES1, and PPT1 for their ability to hydrolyze a fixed amount of 2-AG (final concentration of 10 μM). As shown in Figure 5D, CES1, FAAH, and MAGL hydrolyzed 2-AG *in vitro* at roughly similar rates per mole of enzyme, whereas PPT1 hydrolyzed 2-AG at a rate significantly slower than those of the other enzymes.

Hydrolysis of 2-AG by PPT1: Inhibition by PO, JZL184, and HDSF. To compare the extent of inhibition of PPT1- and CES1-catalyzed hydrolytic activity by the small molecule inhibitors PO, JZL184, and HDSF, the recombinant enzymes were pretreated with each compound for 30 min, followed by addition of 2-AG substrate (final concentration of 10 μM) and incubation for an additional 30 min. As expected,³⁶ Figure 6A shows that PO potently inhibited CES1; however, the PPT1 activity was much less sensitive to PO treatment. This result is reminiscent of the fact that the well-known serine hydrolase inhibitor PMSF also did not block PPT1 enzymatic activity,³⁷ which was attributed to the steric bulk of the phenyl group of PMSF prohibiting access of the electrophilic sulfonyl fluoride

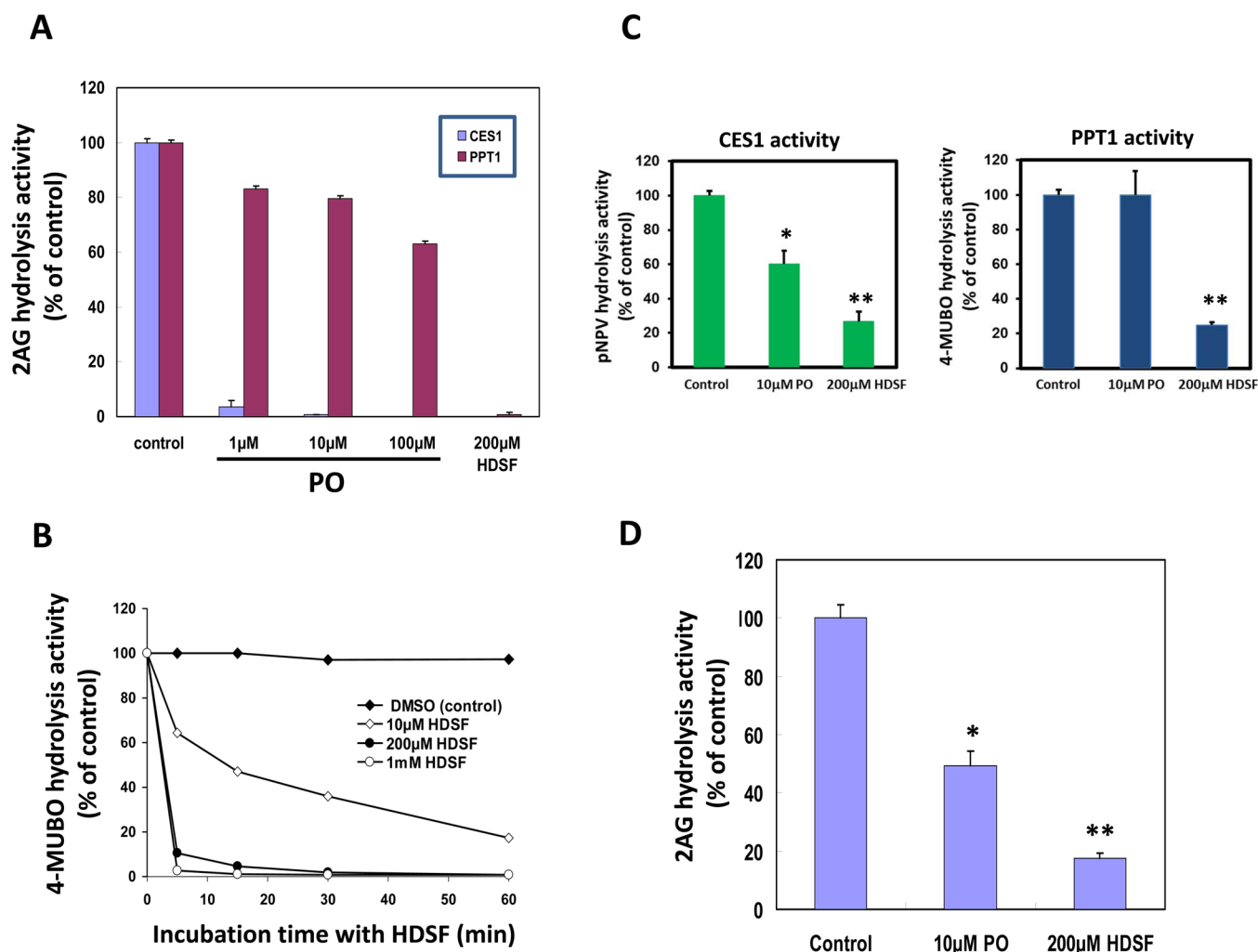


Figure 6. Inhibition of PPT1 by small molecule inhibitors. (A) 2-AG hydrolytic activity of recombinant PPT1 pretreated with 1, 10, and 100 μ M PO or 200 μ M HDSF for 30 min, followed by incubation with 10 μ M 2-AG for an additional 30 min. (B) Time-dependent and concentration-dependent 4-MUBO hydrolysis activity curve of recombinant PPT1 pretreated with HDSF. Recombinant PPT1 was incubated with 10 μ M, 100 μ M, or 1 mM HDSF for different periods of time. (C) Hydrolysis of pNPV (left) and 4-MUBO (right) by cell lysates obtained from THP1 macrophages that had been pretreated with either PO (10 μ M) or HDSF (200 μ M) for 30 min. (D) Hydrolysis of 2-AG by intact THP1 macrophages pretreated with either PO (10 μ M) or HDSF (200 μ M) for 30 min, followed by incubation with 10 μ M 2-AG for 60 min. Data represent means \pm the standard deviation of three independent experiments. * p < 0.05; ** p < 0.01 (Student's t test).

moiety to the narrow catalytic gorge of PPT1. PO would offer steric constraints similar to those of PMSF because of its bulky *p*-nitrophenyl leaving group. In a similar vein, differential inhibition of CES1 and PPT1 was also found for JZL184; CES1 activity was blocked,¹⁰ but PPT1 activity was not (Figure 3A of the Supporting Information). By contrast, 200 μ M HDSF inhibited CES1 and PPT1 activities by nearly 100% (Figure 6A). HDSF inhibited recombinant PPT1 in a time- and concentration-dependent manner, suggesting a covalent mechanism of inhibition (Figure 6B). It is important to note again that HDSF had no effect on cathepsin G on the basis of competitive ABPP (Figure 3A,B of the Supporting Information). In addition, another serine hydrolase, KIAA1363 (also abbreviated NCEH), was detected in THP1 cells by ABPP–MUDPIT (Figure 1A). However, even though recombinant KIAA1363 protein exhibits esterase activity, it does not have lipolytic activity toward 4-MUBO (Figure 5A,B of the Supporting Information), nor can it hydrolyze 2-AG.^{6,28} Furthermore, on the basis of competitive ABPP, 200 μ M HDSF had no effect on KIAA1363 activity in THP1 cell lysates

(Figure 5C of the Supporting Information) or mouse brain extracts (data not shown). Thus, KIAA1363 was probably not the serine hydrolase enzyme that metabolizes 2-AG we were seeking.

We previously investigated the extent of inhibition of CES1 and unknown 31–32 kDa serine hydrolase in whole THP1 monocyte lysates by PO, CPO, and JZL184 using competitive gel-based ABPP.¹⁰ The results indicated CES1 was significantly more sensitive than the unknown 31–32 kDa enzyme,¹⁰ with CES1 exhibiting large k_{inact}/K_i values with these inhibitors.^{36,38} In contrast, high concentrations of PO and CPO (\sim 100 μ M) were needed to modestly impair PPT1 activity (Figure 6A for PO), while JZL184 at concentrations as high as 100 μ M had no effect¹⁰ (and data not shown).

On the basis of these inhibition findings, we designed an experiment to determine the relative contributions of PPT1 and CES1 to 2-AG hydrolysis activity in intact living THP1 monocytes and macrophages. THP1 macrophages were pretreated for 30 min with 10 μ M PO to chemically knock down CES1 activity but leave PPT1 activity essentially intact;

alternatively, 200 μ M HDSF was used to chemically knock down both CES1 and PPT1 activities (Figure 6C). (It was predetermined that this concentration of HDSF did not adversely affect cell viability.) Although the concentration of HDSF used to treat the cells was high, it was necessary to inactivate PPT1 in intact cells (as judged by a decrease in 4-MUBO hydrolysis activity). Furthermore, MAGL, FAAH, ABHD6, and ABHD12 are not present in THP1 cells (Figure 1A) and therefore can be ruled out as off-target enzymes for either PO or HDSF. Following pretreatment with each inhibitor, the cells were exposed to exogenous 2-AG (final concentration of 10 μ M), and the extent of 2-AG hydrolytic metabolism was determined by quantifying the yield of AA. It was discovered that pretreatment with PO and HDSF inhibited 51 and 83% of the 2-AG hydrolytic activity in THP1 macrophages, respectively (Figure 6D). From these data, we estimate that CES1 and PPT1 contribute \sim 51 and \sim 32% of the 2-AG hydrolytic activity in THP1 macrophages, respectively.

Immunodepletion of PPT1 from THP1 Cell Lysates and 2-AG Hydrolysis. Immunoprecipitation of PPT1 from THP1 monocyte lysates using anti-PPT1 antibodies was successfully accomplished on the basis of immunoblots of nonspecific antibody-treated and anti-PPT1 antibody-treated samples (Figure 7A), and the significantly reduced 4-MUBO hydrolytic activity (Figure 7B). Importantly, the hydrolytic activity of the PPT1-depleted lysate toward 2-AG was also markedly reduced by \sim 40% (Figure 7C). These results are consistent with a role for PPT1 in the hydrolysis of 2-AG by THP1 cells. Furthermore, we previously showed that immunodepletion of CES1 from THP1 cell lysates caused an \sim 60% reduction in 2-AG hydrolytic activity,¹⁰ thus complementing the PPT1 immunodepletion results reported here.

DISCUSSION

Noteworthy findings of this study include identification of serine hydrolases in the human THP1 monocyte and macrophage cell line by ABPP–MUDPIT and ABPP–in-gel digest–MUDPIT approaches. One of the identified hydrolases was a serine lipase termed PPT1 (EC 3.1.2.22). It was abundantly expressed in this cell line but was minimally reactive toward the activity-based probe FP-biotin. PPT1 is a monomeric lysosomal hydrolase that metabolizes S-acylated proteins by hydrolyzing thioester bonds that connect long-chain fatty acids of varying lengths (14–18 carbons) to the thiol of cysteine.³⁹ In addition, PPT1 can hydrolyze palmitoyl-CoA and S-palmitoyl thioglucoside and was shown to cleave palmitate from H-Ras proteins.⁴⁰ PPT1 is targeted to lysosomes through the classical mannose 6-phosphate receptor pathway. It was first purified from bovine brain,⁴¹ and its crystal structure revealed a canonical α/β -hydrolase fold typical of lipases, with an essential catalytic triad composed of Ser115, His289, and Asp233.³⁰ Bovine PPT1 is 95% identical to human PPT1 at the amino acid level;⁴² the polypeptide consists of 306 amino acids and a signal sequence of 25 amino acids that is cotranslationally cleaved. We and others found that PPT1 migrates as a doublet or triplet during SDS–PAGE (Figure 1C),⁴³ which collapses to a single \sim 29 kDa protein upon deglycosylation (Figure 1E). PPT1 has three conserved asparagine-linked glycosylation sites at amino acid positions 197, 212, and 232, which are all utilized *in vivo*. The glycan moieties are sensitive to endoglycosidase H, demonstrating that PPT1 possesses only N-type glycosylation. Proper glycosylation is required for the stability and activity of the enzyme,³⁰ and glycosylation site mutants of PPT1 have

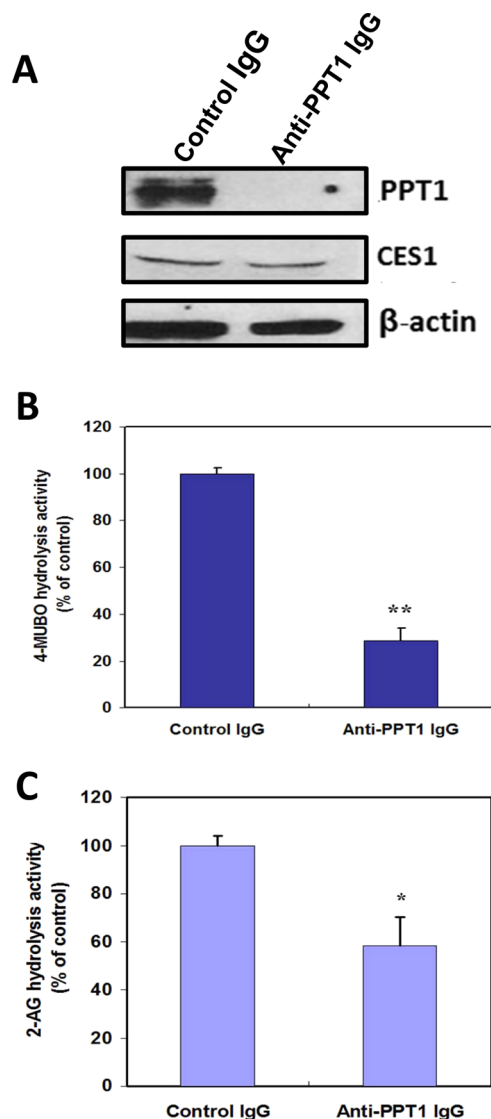


Figure 7. Immunoprecipitation of PPT1 from THP1 monocyte lysates reduces the level of hydrolysis of 2-AG. (A) PPT1 was immunoprecipitated from cell lysates using anti-PPT1 IgG antibodies. As a negative control, lysates were incubated with nonspecific IgG antibodies. Following incubation of whole-cell lysates with antibodies, the antibody–antigen complexes were attached to protein A beads and pelleted by centrifugation. Equivalent amounts of the supernatants were subjected to SDS–PAGE. Immunodepleted supernatants were also subjected to the 4-MUBO hydrolysis activity assay (B) or incubated with 10 μ M 2-AG for 30 min to determine residual 2-AG hydrolytic activity (C). Data represent means \pm the standard deviation of three independent experiments. * p < 0.05; ** p < 0.01 (Student's t test).

greatly reduced enzyme activity.⁴⁴ Interestingly, despite localization of PPT1 in lysosomes, its enzymatic activity is optimal at neutral pH, not pH 4–5⁴⁰ (data not shown). In mammals, PPT1 is found in many different tissues in varying quantities, with the highest levels in the brain, eye, and spleen.^{43,45} In addition to being found in lysosomal compartments of neurons, the protein is also expressed in presynaptic compartments.^{46–48} The expression of PPT1 is under developmental control in the CNS, and it is well-known that loss of PPT1 activity causes a lysosomal storage disorder, which leads to neuronal cell death causing infantile neuronal ceroid lipofuscinoses.^{49,50}

This is the first report that PPT1 is expressed in human THP1 cells and primary monocytes and macrophages. The result is consistent with PPT1 being detected by immunohistochemical approaches in macrophages within human liver, lung, and bowel, but having little or no expression in tissue parenchymal cells.⁵¹ Of the hydrolases currently known to metabolize the endocannabinoid 2-AG, it was interesting that only CES1 was detected in THP1 cells by ABPP–MUDPIT, while MAGL, FAAH, ABHD6, and ABHD12 were undetectable. PPT1 was also expressed in larger amounts than CES1 in THP1 monocytes and macrophages (Figure 3). An unexpected and noteworthy finding was that PPT1 could hydrolyze 2-AG, which is a bioactive lipid with an important role in regulating inflammation in macrophages.³³ In addition, PG-Gs, which are COX-mediated oxygenation products of 2-AG, were also hydrolyzed by PPT1. The catalytic efficiency of 2-AG hydrolysis by recombinant PPT1 is lower (13-fold) than that of CES1 (Table 1). Thus, examination of kinetic parameters suggested that PPT1 is unlikely the major 2-AG hydrolytic enzyme in monocytes and macrophages, but it could have an important auxiliary role in regulating the levels of this endocannabinoid in cell types that do not express MAGL, ABHD6, or ABHD12. The catalytic efficiency for the PPT1–2-AG pair is also in line with the modest catalytic efficiencies observed for enzymes involved in secondary metabolic pathways.⁵² Because PPT1 is primarily found within lysosomes and has a low K_m for 2-AG, it may also regulate distinct pools of lipid glyceryl esters that are either synthesized in or transported to this subcellular compartment. The catalytic efficiency of hydrolysis of 2-AG by pure PPT1 is ~10-fold lower than those of the thioesters palmitoyl-CoA and 4-methylumbelliferyl-6-thiopalmityl- β -D-glucoside,⁵³ which is consistent with the fact that *O*-acyl esters are hydrolyzed slower than thioesters.

Three lines of evidence indicate that CES1 is the major 2-AG hydrolytic enzyme in THP1 cells and PPT1 has an auxiliary role. (i) Fifty-one percent of the 2-AG hydrolytic activity was inhibited by PO, which can inhibit CES1 but not PPT1, whereas 83% was inhibited by HDSF, which can inhibit both CES1 and PPT1 (Figure 6) but not cathepsin G and KIAA1363, which are also expressed in THP1 cells (Figures 3 and 5 of the Supporting Information). Although high concentrations of HDSF are needed to inhibit PPT1 and it is likely HDSF has several off-target enzymes, it is reasonable to rule out MAGL, FAAH, ABHD6, and ABHD12 as off-targets in the context of the THP1 cell line because of their lack of expression. Therefore, 51 and 32% of the 2-AG hydrolytic activity can be attributed to CES1 and PPT1, respectively. These results are consistent with our previous report,¹⁰ which concluded that CES1 accounted for 40–50% of the 2-AG hydrolytic activity in THP1 cells based on the inhibition profile of CES1 chemical inhibitors and CES1 immunodepletion from THP1 cell lysate. (ii) Knockdown of CES1 expression in THP1 cells reduced the 2-AG hydrolytic activity of THP1/CES1 KD cells by 32% relative to that of the control THP1 cells (Figure 2A–C). Although the decrease in 2-AG hydrolytic activity in the CES1-deficient cells did not reach 51%, this could be explained by the fact that PPT1 protein expression appeared to be upregulated in the CES1-deficient cell line compared to the control THP1 cell line. Enhanced PPT1 expression may be a compensatory mechanism following knockdown of CES1 expression, thus contributing to the 2-AG hydrolytic activity of the CES1-deficient cells. (iii) Immunodepletion of PPT1 from THP1 cell lysates reduced 2-AG hydrolytic activity by

~40% (Figure 7), which is similar to the amount estimated using chemical inhibitor HDSF (32%). This result provided strong evidence that PPT1 may have a collaborative role in 2-AG catabolism.

It was also shown in this study that 4-MUBO is an excellent substrate for PPT1 (Figure 4B); pretreatment of intact macrophages with 200 μ M HDSF inhibited nearly 80% of the 4-MUBO hydrolytic activity, whereas 10 μ M PO had no effect (Figure 6C). Because 200 μ M HDSF completely inhibited both PPT1 and CES1, whereas 10 μ M PO completely inhibited CES1 but only minimally affected PPT1 activity (Figure 6A), we interpreted these results to indicate PPT1 was primarily responsible for the 4-MUBO hydrolytic activity of THP1 cells. This conclusion is supported by the markedly reduced 4-MUBO hydrolysis activity of PPT1-depleted cell lysates following immunoprecipitation (Figure 7B). These findings also provided insight into enigmatic results previously reported by us,¹⁴ which showed that high concentrations of organophosphate poisons (oxons) minimally impacted the 4-MUBO hydrolytic activity of THP1 cell lysates. In addition, we observed that 200 μ M PMSF inhibited only ~20% of the 4-MUBO hydrolytic activity of whole-cell lysates (data not shown), which is in line with the fact that PMSF is a poor inhibitor of PPT1.³⁷ Thus, we conclude that PPT1 accounts for the organophosphate- and PMSF-insensitive 4-MUBO hydrolytic activity that we previously observed.¹⁴

In summary, this study confirms and extends several findings of our previous reports,^{10,14} including validation of an *in vivo* role for CES1 in 2-AG metabolism (Figure 2 and Figure 4 of the Supporting Information). It is also the first to identify and quantify palmitoyl protein thioesterase 1 (PPT1) in human THP1 monocytes and macrophages, and the first to show PPT1 can hydrolyze the endogenous cannabinoid 2-arachidonoylglycerol (2-AG) and two prostaglandin glyceryl esters, PGE₂-G and PGF_{2 α} -G, *in vitro*. These findings suggest that PPT1 may also have a role in degrading endocannabinoids in certain cellular niches, especially in cell types lacking or having limited expression of MAGL, FAAH, ABHD6, ABHD12, and CES1. Furthermore, we characterized the hydrolytic efficiency of PPT1 using both 2-AG and PG-G substrates and compared the kinetic parameters to those of CES1, MAGL, and FAAH. We also investigated the relative contributions of PPT1 and CES1 to the hydrolysis of 2-AG in human THP1 cells using chemical inhibitors, immunoprecipitation of PPT1, and knockdown of CES1 expression using a lentiviral shRNA system. Collectively, the results suggest that PPT1 has the ability to recognize and hydrolyze lipid glyceryl esters in human THP1 cells and that PPT1 accounts for ~32% of the 2-AG hydrolytic activity while CES1 contributes ~51%.

There are limitations to this work that should be addressed in future studies, including the need to better characterize the full complement of serine hydrolases in primary human monocytes and macrophages, a need to develop small molecules to overcome the paucity of selective PPT1 inhibitors, and a need to validate the 2-AG hydrolytic activity of PPT1 *in vivo* (e.g., in intact cells and whole animals using knockdown–knockout approaches) by determining whether this enzymatic activity controls the efficacy of 2-AG signaling at cannabinoid receptors. Introduction of shRNA or siRNA constructs into human macrophages is notoriously difficult; we are currently attempting to modulate PPT1 expression in cell lines with viral vectors. However, despite being unable to knock down PPT1 expression in THP1 cells, we did successfully

immunodeplete PPT1 from cell lysates and demonstrate a subsequent reduction (~40%) in 2-AG hydrolysis activity (Figure 7), which complemented the ~60% reduction in 2-AG hydrolysis activity caused by immunodepletion of CES1.¹⁰ Notwithstanding these limitations, the current findings highlight the overlapping substrate specificity and functional redundancy often exhibited by lipases involved in lipid metabolism, and the auxiliary roles certain enzymes such as PPT1 may have in cells. It also potentially opens new avenues of research related to endocannabinoid biochemistry.

■ ASSOCIATED CONTENT

■ Supporting Information

List of identified serine hydrolases in THP1 monocytes, CID fragmentation spectra of one of the identified PPT1 peptides, inhibition of 2-AG hydrolytic activity of THP1 monocyte lysates by FP-biotin, competitive ABPP demonstrating the lack of cathepsin G inhibition in THP1 cell lysates by HDSE, hydrolysis of 2-AG in THP1 macrophages that regulates prostaglandin biosynthesis, and overexpression of human KIAA1363 in COS-7 cells and its esterase and lipase activities. This material is available free of charge via the Internet at <http://pubs.acs.org>.

■ AUTHOR INFORMATION

Corresponding Author

*P.O. Box 6100, Mississippi State University, University, MS 39762. E-mail: mross@cvm.msstate.edu. Phone: (662) 325-5482. Fax: (662) 325-1031.

Funding

This study was supported by National Institutes of Health Grant 1R15ES015348-02 (M.K.R.), and the protein mass spectrometric work was supported by the Mississippi Agricultural and Forestry Experiment Station Special Research Initiatives (M.J.E.) (160000-018100-027100-401120).

Notes

The authors declare no competing financial interest.

■ ACKNOWLEDGMENTS

We thank Dr. Sandra L. Hofmann (University of Texas Southwestern Medical Center) for the kind gift of hPPT1-CHO cells and Dr. Jui-Yun Lu (University of Texas Southwestern Medical Center) for helpful technical advice. We are also grateful to Dr. Phil Potter (St. Jude Children's Research Hospital, Memphis, TN) for providing pure recombinant CES1 protein and Dr. Wei Tan (Mississippi State University) for assistance with peritoneal macrophage isolation. We also thank the Jiangsu Academy of Agricultural Sciences and the Mississippi State University College of Veterinary Medicine for scholarship support to Dr. Ran Wang. Kim Pluta is acknowledged for her role in the KIAA1363 overexpression experiments.

■ ABBREVIATIONS

AA, arachidonic acid; 2-AG, 2-arachidonoylglycerol; ABPP, activity-based protein profiling; CES1, carboxylesterase 1; CPO, chlorpyrifos oxon; HDSE, hexadecylsulfonyl fluoride; 4-MUBA, 4-methylumbelliferyl acetate; 4-MUBO, 4-methylumbelliferyl oleate; MUDPIT, multidimensional protein identification technology; PPT1, palmitoyl protein thioesterase 1; PO, paraoxon; PGE₂-G, prostaglandin E₂ glyceryl ester; PGF_{2α}-G,

prostaglandin F_{2α} glyceryl ester; PMSF, phenylmethanesulfonyl fluoride.

■ REFERENCES

- (1) De Petrocellis, L., Cascio, M. G., and Di Marzo, V. (2004) The endocannabinoid system: A general view and latest additions. *Br. J. Pharmacol.* 141, 765–774.
- (2) Van Sickle, M. D., Duncan, M., Kingsley, P. J., Mouihate, A., Urbani, P., Mackie, K., Stella, N., Makriyannis, A., Piomelli, D., Davison, J. S., Marnett, L. J., Di Marzo, V., Pittman, Q. J., Patel, K. D., and Sharkey, K. A. (2005) Identification and functional characterization of brainstem cannabinoid CB2 receptors. *Science* 310, 329–332.
- (3) Klein, T. W., Newton, C., Larsen, K., Lu, L., Perkins, I., Nong, L., and Friedman, H. (2003) The cannabinoid system and immune modulation. *J. Leukocyte Biol.* 74, 486–496.
- (4) Di Marzo, V. (2009) The endocannabinoid system: Its general strategy of action, tools for its pharmacological manipulation and potential therapeutic exploitation. *Pharmacol. Res.* 60, 77–84.
- (5) Mach, F., and Steffens, S. (2008) The role of the endocannabinoid system in atherosclerosis. *J. Neuroendocrinol.* 20 (Suppl. 1), S3–S7.
- (6) Blankman, J. L., Simon, G. M., and Cravatt, B. F. (2007) A comprehensive profile of brain enzymes that hydrolyze the endocannabinoid 2-arachidonoylglycerol. *Chem. Biol.* 14, 1347–1356.
- (7) Muccioli, G. G., Xu, C., Odah, E., Cudaback, E., Cisneros, J. A., Lambert, D. M., Lopez Rodriguez, M. L., Bajjalieh, S., and Stella, N. (2007) Identification of a novel endocannabinoid-hydrolyzing enzyme expressed by microglial cells. *J. Neurosci.* 27, 2883–2889.
- (8) Marrs, W. R., Blankman, J. L., Horne, E. A., Thomazeau, A., Lin, Y. H., Coy, J., Bodor, A. L., Muccioli, G. G., Hu, S. S., Woodruff, G., Fung, S., Lafourcade, M., Alexander, J. P., Long, J. Z., Li, W., Xu, C., Moller, T., Mackie, K., Manzoni, O. J., Cravatt, B. F., and Stella, N. (2010) The serine hydrolase ABHD6 controls the accumulation and efficacy of 2-AG at cannabinoid receptors. *Nat. Neurosci.* 13, 951–957.
- (9) Navia-Paldanius, D., Savinainen, J. R., and Laitinen, J. T. (2012) Biochemical and pharmacological characterization of human α/β -hydrolase domain containing 6 (ABHD6) and 12 (ABHD12). *J. Lipid Res.* 53, 2413–2424.
- (10) Xie, S., Borazjani, A., Hatfield, M. J., Edwards, C. C., Potter, P. M., and Ross, M. K. (2010) Inactivation of lipid glyceryl ester metabolism in human THP1 monocytes/macrophages by activated organophosphorus insecticides: Role of carboxylesterases 1 and 2. *Chem. Res. Toxicol.* 23, 1890–1904.
- (11) Ross, M. K., Borazjani, A., Wang, R., Crow, J. A., and Xie, S. (2012) Examination of the carboxylesterase phenotype in human liver. *Arch. Biochem. Biophys.* 522, 44–56.
- (12) Ghosh, S. (2000) Cholesteryl ester hydrolase in human monocyte/macrophage: Cloning, sequencing, and expression of full-length cDNA. *Physiol. Genomics* 2, 1–8.
- (13) Quiroga, A. D., and Lehner, R. (2011) Role of endoplasmic reticulum neutral lipid hydrolases. *Trends Endocrinol. Metab.* 22, 218–225.
- (14) Crow, J. A., Middleton, B. L., Borazjani, A., Hatfield, M. J., Potter, P. M., and Ross, M. K. (2008) Inhibition of carboxylesterase 1 is associated with cholesteryl ester retention in human THP-1 monocyte/macrophages. *Biochim. Biophys. Acta* 1781, 643–654.
- (15) Rouzer, C. A., and Marnett, L. J. (2005) Glycerylprostaglandin synthesis by resident peritoneal macrophages in response to a zymosan stimulus. *J. Biol. Chem.* 280, 26690–26700.
- (16) Rouzer, C. A., and Marnett, L. J. (2011) Endocannabinoid oxygenation by cyclooxygenases, lipoxygenases, and cytochromes P450: Cross-talk between the eicosanoid and endocannabinoid signaling pathways. *Chem. Rev.* 111, S899–S921.
- (17) Li, W., Blankman, J. L., and Cravatt, B. F. (2007) A functional proteomic strategy to discover inhibitors for uncharacterized hydrolases. *J. Am. Chem. Soc.* 129, 9594–9595.
- (18) Liu, Y., Patricelli, M. P., and Cravatt, B. F. (1999) Activity-based protein profiling: The serine hydrolases. *Proc. Natl. Acad. Sci. U.S.A.* 96, 14694–14699.

- (19) Borazjani, A., Edelmann, M. J., Hardin, K. L., Herring, K. L., Allen Crow, J., and Ross, M. K. (2011) Catabolism of 4-hydroxy-2-trans-nonenal by THP1 monocytes/macrophages and inactivation of carboxylesterases by this lipid electrophile. *Chem.-Biol. Interact.* 194, 1–12.
- (20) Moellering, R. E., and Cravatt, B. F. (2012) How chemo-proteomics can enable drug discovery and development. *Chem. Biol.* 19, 11–22.
- (21) Lu, J. Y., and Hofmann, S. L. (2006) Thematic review series: Lipid posttranslational modifications. Lysosomal metabolism of lipid-modified proteins. *J. Lipid Res.* 47, 1352–1357.
- (22) Morton, C. L., and Potter, P. M. (2000) Comparison of *Escherichia coli*, *Saccharomyces cerevisiae*, *Pichia pastoris*, *Spodoptera frugiperda*, and COS7 cells for recombinant gene expression. Application to a rabbit liver carboxylesterase. *Mol. Biotechnol.* 16, 193–202.
- (23) Speers, A. E., and Cravatt, B. F. (2009) Activity-Based Protein Profiling (ABPP) and Click Chemistry (CC)-ABPP by MudPIT Mass Spectrometry. *Curr. Protoc. Chem. Biol.* 1, 29–41.
- (24) MacCoss, M. J., Wu, C. C., and Yates, J. R., III (2002) Probability-based validation of protein identifications using a modified SEQUEST algorithm. *Anal. Chem.* 74, 5593–5599.
- (25) Lu, J. Y., Hu, J., and Hofmann, S. L. (2010) Human recombinant palmitoyl-protein thioesterase-1 (PPT1) for preclinical evaluation of enzyme replacement therapy for infantile neuronal ceroid lipofuscinosis. *Mol. Genet. Metab.* 99, 374–378.
- (26) Ross, M. K., and Borazjani, A. (2007) Enzymatic activity of human carboxylesterases. *Current protocols in toxicology*, Chapter 4, Unit 4, 24, Wiley, New York.
- (27) Gupta, P., Soyombo, A. A., Atashband, A., Wisniewski, K. E., Shelton, J. M., Richardson, J. A., Hammer, R. E., and Hofmann, S. L. (2001) Disruption of PPT1 or PPT2 causes neuronal ceroid lipofuscinosis in knockout mice. *Proc. Natl. Acad. Sci. U.S.A.* 98, 13566–13571.
- (28) Bachovchin, D. A., Ji, T., Li, W., Simon, G. M., Blankman, J. L., Adibekian, A., Hoover, H., Niessen, S., and Cravatt, B. F. (2010) Superfamily-wide portrait of serine hydrolase inhibition achieved by library-versus-library screening. *Proc. Natl. Acad. Sci. U.S.A.* 107, 20941–20946.
- (29) Hsu, K. L., Tsuboi, K., Adibekian, A., Pugh, H., Masuda, K., and Cravatt, B. F. (2012) DAGL β inhibition perturbs a lipid network involved in macrophage inflammatory responses. *Nat. Chem. Biol.* 8, 999–1007.
- (30) Bellizzi, J. J., III, Widom, J., Kemp, C., Lu, J. Y., Das, A. K., Hofmann, S. L., and Clardy, J. (2000) The crystal structure of palmitoyl protein thioesterase 1 and the molecular basis of infantile neuronal ceroid lipofuscinosis. *Proc. Natl. Acad. Sci. U.S.A.* 97, 4573–4578.
- (31) Wadkins, R. M., Hyatt, J. L., Wei, X., Yoon, K. J., Wierdl, M., Edwards, C. C., Morton, C. L., Obenaus, J. C., Damodaran, K., Beroza, P., Danks, M. K., and Potter, P. M. (2005) Identification and characterization of novel benzil (diphenylethane-1,2-dione) analogues as inhibitors of mammalian carboxylesterases. *J. Med. Chem.* 48, 2906–2915.
- (32) Nomura, D. K., Morrison, B. E., Blankman, J. L., Long, J. Z., Kinsey, S. G., Marcondes, M. C., Ward, A. M., Hahn, Y. K., Lichtman, A. H., Conti, B., and Cravatt, B. F. (2011) Endocannabinoid hydrolysis generates brain prostaglandins that promote neuroinflammation. *Science* 334, 809–813.
- (33) Alhouayek, M., Masquelier, J., and Muccioli, G. G. (2013) Controlling 2-arachidonoylglycerol metabolism as an anti-inflammatory strategy. *Drug Discovery Today*, DOI: 10.1016/j.drudis.2013.07.009.
- (34) Hedstrom, L. (2002) Serine protease mechanism and specificity. *Chem. Rev.* 102, 4501–4524.
- (35) Vila, A., Rosengarth, A., Piomelli, D., Cravatt, B., and Marnett, L. J. (2007) Hydrolysis of prostaglandin glycerol esters by the endocannabinoid-hydrolyzing enzymes, monoacylglycerol lipase and fatty acid amide hydrolase. *Biochemistry* 46, 9578–9585.
- (36) Crow, J. A., Bittles, V., Herring, K. L., Borazjani, A., Potter, P. M., and Ross, M. K. (2012) Inhibition of recombinant human carboxylesterase 1 and 2 and monoacylglycerol lipase by chlorpyrifos oxon, paraoxon and methyl paraoxon. *Toxicol. Appl. Pharmacol.* 258, 145–150.
- (37) Das, A. K., Bellizzi, J. J., III, Tandel, S., Biehl, E., Clardy, J., and Hofmann, S. L. (2000) Structural basis for the insensitivity of a serine enzyme (palmitoyl-protein thioesterase) to phenylmethylsulfonyl fluoride. *J. Biol. Chem.* 275, 23847–23851.
- (38) Crow, J. A., Bittles, V., Borazjani, A., Potter, P. M., and Ross, M. K. (2012) Covalent inhibition of recombinant human carboxylesterase 1 and 2 and monoacylglycerol lipase by the carbamates JZL184 and URB597. *Biochem. Pharmacol.* 84, 1215–1222.
- (39) Lu, J. Y., and Hofmann, S. L. (2006) Inefficient cleavage of palmitoyl-protein thioesterase (PPT) substrates by aminothiols: Implications for treatment of infantile neuronal ceroid lipofuscinosis. *J. Inherited Metab. Dis.* 29, 119–126.
- (40) Verkruijse, L. A., and Hofmann, S. L. (1996) Lysosomal targeting of palmitoyl-protein thioesterase. *J. Biol. Chem.* 271, 15831–15836.
- (41) Camp, L. A., and Hofmann, S. L. (1993) Purification and properties of a palmitoyl-protein thioesterase that cleaves palmitate from H-Ras. *J. Biol. Chem.* 268, 22566–22574.
- (42) Schriener, J. E., Yi, W., and Hofmann, S. L. (1996) cDNA and genomic cloning of human palmitoyl-protein thioesterase (PPT), the enzyme defective in infantile neuronal ceroid lipofuscinosis. *Genomics* 34, 317–322.
- (43) Isosomppi, J., Heinonen, O., Hiltunen, J. O., Greene, N. D., Vesa, J., Uusitalo, A., Mitchison, H. M., Saarma, M., Jalanko, A., and Peltonen, L. (1999) Developmental expression of palmitoyl protein thioesterase in normal mice. *Brain Research and Developmental Brain Research* 118, 1–11.
- (44) Lyly, A., von Schantz, C., Salonen, T., Kopra, O., Saarela, J., Jauhainen, M., Kytälä, A., and Jalanko, A. (2007) Glycosylation, transport, and complex formation of palmitoyl protein thioesterase 1 (PPT1): Distinct characteristics in neurons. *BMC Cell Biol.* 8, 22.
- (45) Suopanki, J., Tyynelä, J., Baumann, M., and Haltia, M. (1999) The expression of palmitoyl-protein thioesterase is developmentally regulated in neural tissues but not in nonneural tissues. *Mol. Genet. Metab.* 66, 290–293.
- (46) Heinonen, O., Kytälä, A., Lehmus, E., Paunio, T., Peltonen, L., and Jalanko, A. (2000) Expression of palmitoyl protein thioesterase in neurons. *Mol. Genet. Metab.* 69, 123–129.
- (47) Lehtovirta, M., Kytälä, A., Eskelinen, E. L., Hess, M., Heinonen, O., and Jalanko, A. (2001) Palmitoyl protein thioesterase (PPT) localizes into synaptosomes and synaptic vesicles in neurons: Implications for infantile neuronal ceroid lipofuscinosis (INCL). *Hum. Mol. Genet.* 10, 69–75.
- (48) Ahtainen, L., Van Diggelen, O. P., Jalanko, A., and Kopra, O. (2003) Palmitoyl protein thioesterase 1 is targeted to the axons in neurons. *J. Comp. Neurol.* 455, 368–377.
- (49) Vesa, J., Hellsten, E., Verkruijse, L. A., Camp, L. A., Rapola, J., Santavuori, P., Hofmann, S. L., and Peltonen, L. (1995) Mutations in the palmitoyl protein thioesterase gene causing infantile neuronal ceroid lipofuscinosis. *Nature* 376, 584–587.
- (50) Goebel, H. H., and Wisniewski, K. E. (2004) Current state of clinical and morphological features in human NCL. *Brain Pathol.* 14, 61–69.
- (51) Margraf, L. R., Boriack, R. L., Routheut, A. A., Cuppen, I., Alhaili, L., Bennett, C. J., and Bennett, M. J. (1999) Tissue expression and subcellular localization of CLN3, the Batten disease protein. *Mol. Genet. Metab.* 66, 283–289.
- (52) Bar-Even, A., Noor, E., Savir, Y., Liebermeister, W., Davidi, D., Tawfik, D. S., and Milo, R. (2011) The moderately efficient enzyme: Evolutionary and physicochemical trends shaping enzyme parameters. *Biochemistry* 50, 4402–4410.
- (53) Das, A. K., Lu, J. Y., and Hofmann, S. L. (2001) Biochemical analysis of mutations in palmitoyl-protein thioesterase causing infantile

and late-onset forms of neuronal ceroid lipofuscinosis. *Hum. Mol. Genet.* 10, 1431–1439.